haematologica
Journal of the Ferrata Storti Foundation

EZH2 inhibition overcomes immunomodulatory drug resistance in multiple myeloma via a cereblon-dependent pathway

by Yigen Li, Amy Wilson, Yakinthi Chrisochoidou, Shannon Martin, Sarah Bird, Salomon Morales, Marc Leiro, Zuza Kozik, Nicholas T. Crump, Theodoros I. Roumeliotis, Jyoti Choudhary and Charlotte Pawlyn

Received: April 12, 2025.
Accepted: January 29, 2026.

Citation: Yigen Li, Amy Wilson, Yakinthi Chrisochoidou, Shannon Martin, Sarah Bird, Salomon Morales, Marc Leiro, Zuza Kozik, Nicholas T. Crump, Theodoros I. Roumeliotis, Jyoti Choudhary and Charlotte Pawlyn. EZH2 inhibition overcomes immunomodulatory drug resistance in multiple myeloma via a cereblon-dependent pathway.
Haematologica. 2026 Feb 12. doi: 10.3324/haematol.2025.288024 [Epub ahead of print]

EZH2 inhibition overcomes immunomodulatory drug resistance in multiple myeloma via a cereblon-dependent pathway

Yigen Li[1]*, Amy Wilson[1]*, Yakinthi Chrisochoidou[1], Shannon Martin[1], Sarah Bird[1,2], Salomon Morales[1], Marc Leiro[1], Zuza Kozik[1], Nicholas T. Crump[3], Theodoros I. Roumeliotis[1], Jyoti Choudhary[1], Charlotte Pawlyn[1,2]

1. The Institute of Cancer Research, London
2. The Royal Marsden Hospital NHS Foundation Trust, London
3. Hugh and Josseline Langmuir Centre for Myeloma Research, Centre for Haematology, Department of Immunology and Inflammation, Imperial College London, London
*Joint first authors

Corresponding author:
Dr Charlotte Pawlyn
The Institute of Cancer Research
London, SM2 5NG. UK
charlotte.pawlyn@icr.ac.uk
02087224000

Running Title: EZH2 inhibition overcomes IMiD/CELMoD resistance

Keywords: multiple myeloma, IMiDs, CELMoDs, CRBN, IRF4, EZH2, Tazemetostat, synergistic cell death, IMiD/CELMoD resistance

Data sharing:
The mass spectrometry proteomics data have been deposited to the ProteomeXchange Consortium via the PRIDE partner repository with the dataset identifier PXD057933.

Disclosure/Conflicts of Interest:
The ICR has a commercial interest in the development of compounds targeting CRL4-CRBN E3-ubiquitin ligases. CP has received honoraria from Celgene/BMS (manufacturer of IMiDs/CELMoDs) for advisory boards, educational talks and participation in data monitoring committees. CP has also received honoraria for advisory boards and/or educational talks from Abbvie, Amgen, Takeda, Sanofi, iTEOS, Pfizer, Menarini Stemline, Opna Bio. All other authors have no relevant conflicts of interest to declare.

Contributions:
YL, AB, and CP conceived aspects of the project and designed the analysis; YL, AB, YC, SMa, SB, SMo and ML conducted wet-lab experiments; YL, AB and YC carried out data analysis; NC provided advice and primers for ChIP; ZK, TR and JC conducted and/or supervised the proteomics experiment; YL and CP drafted the paper. All authors contributed to critically revising the paper and approved the final submitted version.

Funding:
This work was primarily funded by a CRUK Clinician Scientist Fellowship grant [C47608/A29957] to CP and supported by additional funding from CRIS Cancer and The Institute of Cancer Research.

Acknowledgement:

We acknowledge the support of The Centre for Protein Degradation and The Centre for Cancer Drug Discovery at The Institute of Cancer Research, specifically Dr John Caldwell and Dr Alice Harnden for compound synthesis. We acknowledge the support of the Flow Cytometry and Proteomics Core Facilities at The Institute of Cancer Research.

Abstract

Immunomodulatory agents (IMiDs) and the next-generation Cereblon (CRBN) E3 ligase modulators (CELMoDs), targeting the IKZF1/IKZF3-IRF4-MYC axis, are effective therapies for multiple myeloma (MM) across all stages of disease. Resistance to treatment can be acquired following exposure, but a subset of patients have primary resistance, with both states necessitating the development of alternative treatment strategies. Enhancer of zeste homolog 2 (EZH2) has been shown to have increased expression at myeloma relapse and higher expression is associated with a shorter progression free survival from diagnosis. EZH2 inhibitors have been studied as a single agent in myeloma and in combination treatments to overcome drug resistance in other malignancies. In this study KMS-11 and RPMI-8226 myeloma cell lines are used as models of primary IMID resistance, demonstrating persistent Interferon regulatory factor 4 (IRF4) expression after IMiDs/CELMoDs exposure without loss of cell viability. The combination of Tazemetostat, an FDA-approved EZH2 inhibitor, with IMiDs/CELMoDs significantly reduces IRF4 expression, induces apoptosis, and leads to synergistic cell death in these resistant cell lines. Further investigations reveal that the synergistic effect of EZH2 inhibition appears specific to IMiDs/CELMoDs, is CRBN-dependent and rescued by IRF4 overexpression. Mechanistically, Tazemetostat appears to reduce IKZF1 binding to the *IRF4* promoter and super-enhancer, explaining how the combination with IMiDs/CELMoDs which also have this effect may reach the threshold required to suppress IRF4 expression and ultimately inhibit MM cell growth in resistant cell lines. Our findings highlight a potential strategy for treating MM patients with IMiD resistance.

Introduction

Multiple myeloma (MM) is a hematologic malignancy characterized by the clonal proliferation of plasma cells in the bone marrow, accounting for approximately 2% of cancers and about 10% of all hematologic malignancies. As the median age of onset is around 70 years there has been a 38% increase in incidence rates since the early 1990s as the population ages[1]. Immunomodulatory drugs (IMiDs), such as Lenalidomide (Len) and Pomalidomide (Pom) have significantly improved patients' survival[2], and the next-generation Cereblon (CRBN) E3 ligase modulators (CELMoDs), including Iberdomide (Iber) and Mezigdomide (Mezi) are currently in Phase III clinical trials. IMiDs/CELMoDs act as molecular glues binding CRBN, a substrate receptor in the CRBN-CRL4 E3 ubiquitin ligase complex[3, 4]. This interaction alters CRBN's substrate affinity, leading to the ubiquitination and degradation of two key B-cell transcription factors, IKZF1 (Ikaros) and IKZF3 (Aiolos) (**Figure 1A**)[4-6]. This degradation leads to the downregulation of the IRF4-MYC axis, which is essential for myeloma pathogenesis, and so ultimately inhibits MM cell proliferation. Resistance to treatment can be acquired following exposure. The mechanisms underlying this acquired resistance are heterogeneous, including CRBN mutations and decreased CRBN expression in some but not all patients[7]. A subset of patients has primary or intrinsic resistance to these agents without prior exposure, around 25-40% to Lenalidomide used in early line therapy[8, 9]. The mechanisms underlying this and to what extent acquired resistance may be reflective of the selection of intrinsically resistant subclones rather than a de novo acquired state, is less well understood, but genetic alteration of CRBN or modified expression is unlikely to be responsible for intrinsic resistance[10]. Studying the underlying reasons for resistance and how it can be overcome, may allow combination treatment approaches to mitigate this challenge.

IRF4 is a critical dependency in myeloma, and its inhibition leads to MM cell death[11]. The primary mechanisms by which IRF4 contributes to MM pathogenesis are through the IRF4-MYC auto-regulatory oncogenic feedback loop and IRF4 self-regulatory feedback loop[12]. Therefore, targeting

the IRF4-MYC axis presents significant challenges as compensatory mechanisms to maintain expression by transcriptional rewiring can arise[13, 14].

Enhancer of zeste homolog 2 (EZH2), a catalytic subunit of the Polycomb Repressive Complex 2 (PRC2), mediates histone H3 methylation at lysine 27 (H3K27me3), resulting in transcriptional repression [15, 16]. Its role in cancer initiation, progression, and drug resistance has been extensively reviewed[17]. EZH2 is frequently overexpressed in MM, associated with poor prognosis[18-20]. In the DREAM challenge analysis, one of the genes whose expression had the highest concordance with shorter progression-free survival (PFS) was PHF19, which directly regulates the PRC2 complex by binding to H3K36me3 and leading to activation of EZH1/2 and H3K27me3[21]. EZH2 itself was also highly correlated. At the DNA level, EZH2 mutations have been identified as a novel driver at relapse with a significant enrichment in events including increased frequency of new mutations and increased cancer cell fraction (CCF) of previously identified mutations[22].

Preclinical studies have shown that EZH2 inhibition can suppress oncogenes and restore tumour suppressor gene expression in MM models[19, 23, 24]. Tazemetostat, the first-in-class EZH2 inhibitor (EZH2i), is approved by the FDA for the treatment of follicular lymphoma and epithelioid sarcoma. The combination of EZH2i with other drugs may yield synergistic effects by simultaneously targeting multiple pathways involved in MM pathogenesis[25, 26]. The combination of 5-azacytidine and EZH2i was shown to restore sensitivity to IMiDs in acquired resistance MM cell lines[27]. In the same study, a suggestion that EZH2i alone may lead to sensitization to Lenalidomide and Pomalidomide was raised but not further explored. No studies to date have fully investigated the efficacy of the Tazemetostat and IMiDs/CELMoDs combination in overcoming primary resistance to IMiDs/CELMoDs in MM, or explored the underlying mechanism.

Here, we investigated the role of EZH2 inhibition in overcoming primary IMiD/CELMoD resistance using MM cell line models. Our findings provide new insights into the interplay between epigenetic regulation and IMiD/CELMoD sensitivity and suggest a novel approach to treating resistant MM.

Materials and methods

Cell culture and generation of stable cell lines

Human multiple myeloma cell lines, AMO-1, NCI-H929, L363, LP1, MM.1S, MOLP-8, U266, RPMI-8226 and KMS-11 were cultured in RPMI-1640 (61870, Gibco) supplemented with 10% Fetal Bovine Serum (FBS) (A5256801, Gibco) and 50 U/ml penicillin/streptomycin (15140122, Gibco) in a humidified 37°C incubator with 5% CO2. To generate CRBN knockout (KO) cells, six sgRNA sequences (TAAACAGACATGGCCGGCGA, GTCCTGCTGATCTCCTTCGC, ATATGCCTATCGAGAAGAAC, ATAGTACCTAGGTGCTGATA, CGCACCATACTGACTTCTTG, AAAATCCTGTTCTTCTCGAT) targeting CRBN exons 1-4 were cloned into pSpCas9-BB-2A-GFP (PX458, Addgene #48138)[28] and plasmids were pooled. Plasmids were transfected into the parental KMS-11 cell line using the Nucleofector kit V (Lonza) and the Amaxa Nucleofector Technology (Lonza) with G-016 pulsing parameters. Transfected cells were maintained for 48h prior to isolating GFP+ cells *via* FACs (SH800 Cell Sorter, Sony) and single cell seeding to generate clonal cell lines. Successful KO was validated post cell line recovery by RT-qPCR (TaqMan Gene expression probes Hs01020593_m1, Hs00372266_m1, Hs00372271_m1, Thermo Fisher Scientific), as well as immunoblotting (CRBN, D8H3S, CST). Re-expression of CRBN mutations (or wild-type CRBN) was performed in KMS-11 and MM.1S cell lines as previously described [29].

Codon-optimized IRF4 (from gBlocks (IDT)) was cloned into pLenti-CMV-GFP-hygro (656-4, Addgene, #17446) between XbaI and BamHI and was lenti-virally transduced into KMS-11 to generate IRF4-GFP overexpressing cells. Cells were selected by Hygromycin (250µg/ml) and sorted by flow cytometry based on GFP expression. The success of viral transduction was validated by detecting codon-

optimized *IRF4* mRNA using RT-qPCR (exoIRF4 #1F, ACGATCTCAGTTGGACATAAGTG; #1R, GCTCGGATAAGGTGTAGTCATC; #2F, TCTTAGTGAGCTCCAAGCATTC; #2R, TGATATGTGCTCGGGAAGGTCA), and WB.

Cell viability assay

Cell viability assay was employed to evaluate cell viability affected by EZH2 inhibitor (EZH2i) or IMiDs as a single reagent or combination. Briefly, if treated with a single reagent, cells were seeded and treated in a 96-well plate and incubated for 120h. For drug combinations, cells were primed in DMSO or Tazemetostat for 120h, followed by re-seeding into a 96-well plate with continued exposure to DMSO/Tazemetostat and IMiD/CELMoD concentrations for a further 120h. For siRNAs, cells were treated with siRNAs in 12-well plate for 96h and were then reseeded in 96-well plate and incubated for 72h. Cell viability was then measured by CellTiter-Blue (G8081, Promega) according to the manufacturer's instructions. Relative cell viability was calculated by normalizing each treatment condition to its respective controls except where otherwise indicated. Synergy score for drug combination was calculated by using SynergyFinder+[30].

Proteomics

KMS-11 cells were incubated in 0.25μM Tazemetostat or DMSO for 10 days and then in combination with 8μM Pomalidomide or DMSO for 24h. Proteomics analysis was performed as previously described[31] with further details in the **Supplementary Methods**. Differentially expressed proteins (DEPs) were identified using DEP package[32] in R (4.4.1). $|\text{Log}_2\text{fold change}| > 0.5$ and p.adj < 0.05 were used to determine significance.

Statistical Analysis

Statistical analysis was performed using GraphPad Prism 10.30. Student's t-test (unpaired, two-tailed) was performed to determine significance when comparing data from different groups.

Methods for siRNA, Western blotting, RNA analysis, apoptosis assays, ChIP-qPCR and proteomics are given in the **Supplementary Methods**. This work followed research integrity and ethical standards appropriate to a laboratory study in the UK.

Results

Persistent IRF4 expression is associated with primary IMiD/CELMoD resistance

To assess IMiD/CELMoD resistance, a panel of MM cell lines representing the inherent molecular heterogeneity of disease were treated with Lenalidomide, Pomalidomide or Iberdomide at various concentrations for 5 days and the IC50 was calculated (**Table S1**). MM.1S and NCI-H929 demonstrated the greatest sensitivity to IMiDs/CELMoDs, as evidenced by reduced cell viability at Day 5 compared to other cell lines, while RPMI-8226 and KMS-11 exhibited the greatest resistance (**Figure 1B**). No clear correlation was observed between resistance and the expression of proteins involved in the CRBN pathway (**Figure 1C**) or with molecular subtype of disease (**Table S2**) (adapted from Keats Lab[33]). Consequently, RPMI-8226 and KMS-11 were selected as the resistant cell line models for the study (**Figure 1D**).

The primary action of IMiDs/CELMoDs is the degradation of IKZF1/IKZF3 and subsequent downregulation of IRF4 expression within the CRBN pathway. To investigate this effect, MM.1S, KMS-11, and RPMI-8226 were treated with Lenalidomide, Pomalidomide and Iberdomide. Results demonstrated all three drugs led to IKZF1/IKZF3 degradation (**Figure 1E, F**). However, significant IRF4 reduction was only observed in MM.1S, a sensitive cell line, not in KMS-11 and RPMI-8226. To confirm that IRF4 remained a key vulnerability in the IMiD resistant state[12], KMS-11 and RPMI-8226 cells were treated with siIRF4 for 5 days, after which cell viability was measured (**Figure 1G, H**). Depletion of IRF4 significantly reduced cell viability in these cell lines, indicating that IRF4 was

essential for KMS-11 and RPMI-8226 cell growth and suggesting its persistent expression contributed to primary IMiD/CELMoD resistance.

EZH2 inhibition overcomes IMiD/CELMoD resistance

To investigate the effect of combining epigenetic modification by EZH2i and IMiDs/CELMoDs on resistant cell lines, the optimal concentration of Tazemetostat was identified to demonstrate on target activity (reduction in H3K27me3) whilst maintaining cell survival (without significant single agent activity), based on the dose-response curve of Tazemetostat (**Figure S1**). Cells were initially primed with Tazemetostat for 5 days and then treated with Pomalidomide or Iberdomide for an additional 5 days in the continued presence of Tazemetostat (**Figure 2A**). The results showed that Tazemetostat and IMiD/CELMoD combination significantly reduced cell viability in resistant cell lines compared to cells treated with IMiD/CELMoD monotherapy (**Figure 2B**), suggesting EZH2i could overcome IMiD/CELMoD resistance. Apoptosis was significantly enhanced in KMS-11 and RPMI-8226 cell lines with the combination treatment compared to Pomalidomide monotherapy, at both Day 5 and Day 3 following Pomalidomide exposure (**Figure 2C, D; Figure S2, S3**).

EZH2 inhibition is synergistic with IMiD/CELMoDs

To explore whether the combined effect of EZH2i with different IMiDs/CELMoDs exceeded the sum of their individual effects, synergy scores were calculated using the Bliss Model in SynergyFinder+[30]. A synergy score above 10 is considered indicative of a synergistic drug combination. Synergy scores of the Tazemetostat-Pomalidomide combination were 8.43, 10.76 and 13.51 in MM.1S, KMS-11 and RPMI-8226 respectively (**Figure 3A**), suggesting that the drug combination was synergistic in resistant MM cell lines. The synergy of Tazemetostat with other IMiD/CELMoD was further investigated in KMS-11. Lenalidomide, which has the lowest CRBN binding potency, showed no synergy (1.08) with Tazemetostat (**Figure 3B**). Iberdomide and Mezigdomide, which have stronger CRBN binding potency, exhibited higher synergy scores (15.66 and 34.53 respectively) (**Figure 3B**).

These results suggested that increased CRBN binding potency correlates with enhanced synergy with Tazemetostat.

The synergy of EZH2i with other drugs used in MM therapy was also evaluated. Dexamethasone demonstrated synergy with Tazemetostat (Bliss score 16.14), but all other tested drugs (Cyclophosphamide, Melphalan, Bortezomib and Doxorubicin) did not (**Figure S4**). Taken together, our results suggested that the Tazemetostat-IMiD/CELMoD combinations were synergistic in resistant cell lines and this synergy was specific to IMiDs/CELMoDs and dexamethasone.

EZH2 inhibition overcomes IMiD/CELMoD resistance in a CRBN-dependent manner

The association between increased CRBN binding potency and enhanced synergy with Tazemetostat suggested a key role for CRBN-related degradation. One hypothesis considered was that Tazemetostat may alter the neo-substrate degradation profile induced by IMiDs. To explore this, proteomic analysis was performed and differentially expressed proteins between conditions compared. Known neo-substrates, such as IKZF1, IKZF3 and ZFP91[34], were downregulated in cells treated with Pomalidomide alone ($|Log_2FC|>0.5$, p.adj<0.05, **Figure 4A** left). This pattern was not caused by Tazemetostat alone (**Figure 4A** mid-left), or altered by the addition of Tazemetostat (**Figure 4A** mid-right), suggesting no direct alteration of neo-substrate degradation was induced. However, the combination of Tazemetostat and Pomalidomide resulted in 43 significantly downregulated proteins (DRPs) and 130 significantly upregulated proteins (URPs) compared to control cells (**Figure 4B**). Enriched pathways associated with downregulated proteins included ferroptosis, pyrimidine metabolism and p53 signalling; enriched pathways associated with upregulated proteins included cytoskeleton in muscle cells, proteoglycans in cancer and arrhythmogenic right ventricular cardiomyopathy (**Figure S5**). IRF4 was downregulated only in the Tazemetostat-Pomalidomide combination, but not in cells treated with Tazemetostat alone or Pomalidomide alone (**Figure 4A, B**). WB analysis further confirmed that only Tazemetostat-Pomalidomide combination reduced IRF4 expression in resistant cell lines (**Figure 4C**).

An isogenic KMS-11 cell line with CRBN knockout (KO) was generated to investigate the role of CRBN in the Tazemetostat-IMiDs/CELMoDs drug combination (**Figure S6**). Cell viability assays demonstrated that the KO completely abrogated the effect of the combination both in terms of cell viability and decreased IRF4 expression (**Figure 4D-F**), indicating that CRBN expression is critical for the combination effect. Supporting this, experiments in MM.1S cell line generated with acquired resistance to Iberdomide, with low but not absent CRBN expression, responded to the Tazemetostat combination but only with CELMoDs rather than the less potent IMiDs (**Figure S7**) and to a greater extent with Mezigdomide than Iberdomide. Resistant cell lines with no detectable CRBN expression behaved like the CRBN KO. Further experiments were conducted in cell lines engineered to express key CRBN mutations in the CRBN KO background, to simulate another IMiD resistance mechanism previously identified in patients. Re-expression of wild-type (WT) CRBN resulted in synergy between Tazemetostat and Pomalidomide or Iberdomide (**Figure S8**) whilst mutations known to completely abrogate CRBN function through mutation of the thalidomide binding domain (e.g. p.W386A) showed no significant synergy further highlighting the key role for functional CRBN in the synergistic effect. Consistent with our previous findings, Tazemetostat appeared to act synergistically with Iberdomide but not Pomalidomide in the presence of the p.C326G mutation [29].

IRF4 overexpression partially rescues the synergistic effect of the Tazemetostat-IMiD/CELMoD combination

The key role of IRF4 in the CRBN dependent synergy demonstrated between Tazemetostat and IMiDs/CELMoDs was explored further. GFP-tagged IRF4 (codon-optimised) was overexpressed in KMS-11 cell line, and the overexpression of exogenous IRF4 was confirmed by qPCR and WB (**Figure S9**). In this model the expression of exogenous IRF4 was driven by the CMV promoter, rather than the native IKZF1/IKZF3 binding promoter and the effect of the Tazemetostat-IMiD/CELMoD combination on altered IRF4 expression was ameliorated as the result of IRF4 self-regulatory function (**Figure 5A, B**). In addition, compared to the control cell line, exogenous expression of IRF4 partially rescued the MYC reduction (**Figure 5C**) and therefore the effect of Tazemetostat-

IMiD/CELMoD combination on cell proliferation (**Figure 5D**). These results indicated that the synergy between Tazemetostat and IMiDs/CELMoDs was, at least partially, mediated by IRF4 downregulation.

Tazemetostat reduces IKZF1 enrichment within the IRF4 promoter and enhancer

Given that EZH2i epigenetically modifies chromatin and gene transcription, the impact of the drug combination on *IRF4* mRNA level was analyzed. IMiD/CELMoD treatment alone significantly reduced *IRF4* mRNA expression in the sensitive cell line MM.1S, whereas it had limited effect on *IRF4* expression in resistant cell lines (**Figure 6A**). Combined with the protein data (**Figure 1E, F**), these findings suggested that *IRF4* mRNA expression was not transcriptionally regulated by IMiDs-CRBN-mediated IKZF1/IKZF3 degradation in the resistant setting. Expression of *IRF4* mRNA was, however, reduced by the combination treatment and this reduction was CRBN-dependent (**Figure 6B**), suggesting that Tazemetostat might epigenetically modify the resistant cell lines leading to restoration of transcriptional regulation of *IRF4* mRNA expression by IKZF1/IKZF3.

To further investigate, *IRF4* mRNA expression and its epigenetic regulation was examined in cells treated with Tazemetostat alone. Tazemetostat had no significant impact on reducing *IRF4* mRNA and protein expression in KMS-11, but significantly reduced *IRF4* mRNA and protein expression in RPMI-8226 (**Figure 6C, D**). This finding was consistent with the cell viability data, which indicated that RPMI-8226 was somewhat sensitive at higher concentrations to Tazemetostat alone (**Figure S1**). ChIP-qPCR analysis in KMS-11 showed that Tazemetostat significantly reduced H3K27me3 enrichment at the *IRF4* promoter (**Figure 6E**). This finding suggested that Tazemetostat altered the chromatin compaction at the *IRF4* promoter, which might be expected to increase gene expression. However, the results showed either unchanged or reduced *IRF4* mRNA expression in KMS-11 and RPMI-8226, respectively (**Figure 6C, D**). Since IKZF1/IKZF3 are key transcriptional factors for *IRF4* known to bind at both the promoter and upstream super-enhancer (SE) region within *DUSP22*[14, 35-37], ChIP-qPCR to assess IKZF1 binding to both these sites was performed. Three pairs of primers were

used to detect different regions of the *IRF4* promoter and three at the SE (**Figure 6F, G**). For the promotor, primer #1 detected a known IKZF1 binding region[35], while primers #2 and #3 targeted putative binding sites predicted by JASPAR[38]. For the enhancer primers SE1-3 targeted peaks of H3K27ac within the SE. The results showed an apparent reduction in IKZF1 enrichment at the *IRF4* promoter and enhancer, with greater binding and reduction in binding seen at the enhancer (**Figure 6F, G**).

These results suggested that the synergistic Tazemetostat-IMiD/CELMoD combination significantly reduced IRF4 transcription *via* resensitizing cells to IMiDs-CRBN-mediated IKZF1/IKZF3 degradation. Mechanistically, Tazemetostat reduced IKZF1 binding to the IRF4 promoter. Based on this, we propose a model for how the Tazemetostat-IMiDs/CELMoDs combination could overcome drug resistance (**Figure 6H**). Alteration of IKZF1/IKZF3 at the *IRF4* promotor and/or enhancer regions by either Tazemetostat or IMID/CELMoD as single agents is insufficient to alter *IRF4* expression enough to result in cell death. In contrast, exposure to EZH2 inhibition modulates transcriptional control of *IRF4* expression to an extent that IMID/CELMoD mediated degradation of IKZF1/IKZF3 leads to reduced *IRF4* expression, resulting in the synergistic effect and cell death.

Discussion

Despite significant improvements in outcomes for patient with MM over the last few decades, precipitated by novel therapies including IMiDs, therapy resistance remains an ongoing challenge. Newer agents including the more potent CELMoDs are demonstrating efficacy in relapsed refractory disease, but patients continue to inevitably relapse and so approaches to address the resistant state are needed to improve outcomes for patients.

In this study, we demonstrate that KMS-11 and RPMI-8226 myeloma cell lines exhibit resistance to IMIDs/CELMoDs with persistent *IRF4* expression despite expression of functional CRBN and degradation of IKZF1 and IKZF3. Reducing *IRF4* expression has been shown to inhibit the proliferation

of MM cells and multiple effective anti-myeloma therapeutics have this downstream result[12, 39]. We demonstrate IRF4 dependency is maintained in KMS-11 and RPMI-8226 with depletion of IRF4 significantly reducing cell viability. This supports the findings of other studies recently reported that suggest transcriptional plasticity as an underlying route to IMiD resistance[13, 14] with studies showing that c-FOS/c-JUN, BATF or ETV4 could substitute for IKZF1/IKZF3 to maintain *IRF4* expression and confer resistance[13, 14, 40].

Epigenetic aberrations are closely associated with the pathogenesis of MM and are considered as a mechanism for drugs (including IMiDs) resistance[41-43]. Two key recent studies highlight the role of EZH2 in myeloma treatment resistance and relapse[21, 22], but the effects of EZH2 inhibition to overcome this has not been well explored. Our results show that Tazemetostat-IMiD/CELMoD drug combinations led to a reduction of IRF4 expression and significantly induced cell death *via* apoptosis, compared to IMiDs/CELMoDs monotherapy in the intrinsically resistant cell lines. Determining the synergy score between Tazemetostat and each of the IMiD/CELMoD agents, we observed that synergy increased with the potency of CRBN binding. This finding suggested that the synergy effect of drug combination is CRBN-dependent which we confirmed using a knock-out model. Furthermore, our results demonstrate that Tazemetostat does not exhibit synergy with the majority of conventional drugs used in MM treatment (with the exception of dexamethasone), suggesting the synergy is largely specific to IMiDs/CELMoDs. Our proteomic analysis and subsequent validation demonstrated that only the drug combination significantly reduced IRF4 expression and led to cell death which could be partially rescued by IRF4 overexpression.

A recent study reported the use of 5-azacytidine and/or Tazemetostat to restore sensitivity to IMiDs in acquired resistant models (to Lenalidomide and Pomalidomide) and concluded this effect was not mediated by increasing CRBN expression[27]. This is consistent with our findings; their acquired resistant cells maintained low level (not absent) CRBN expression. We also expanded further on their

findings in acquired resistance by analysing the effect of the combination in CELMoD (Iberdomide) resistant cell lines with very low CRBN expression.

Our study focusses on intrinsic or primary resistance mechanisms to IMiDs/CELMoDs as the cell lines studied were derived from patients prior to IMiD/CELMoD introduction to the clinic. Primary resistance remains an important clinical problem in itself, and also may reflect the mechanism by which a subclone of cells leads to relapse in patients following therapy, or acquired resistance. It is currently not clear what proportion of patients at relapse have mechanisms similar to those of primary resistance versus those associated with genetic alteration or transcriptional downregulation seen only following exposure i.e. acquired resistance after treatment. Here we demonstrate that CRBN expression is required for EZH2i and IMiD/CELMoD synergy but even low levels of CRBN may be sufficient, especially with the more potent CELMoDs, such as Iberdomide and Mezigdomide, meaning this approach may be relevant for both states. Additionally, we explored the impact on EZH2i and IMiD CELMoD synergy in the presence of mutations of CRBN. This highlights the need for functional CRBN (without mutations that completely abrogate E3 ligase activity) for synergy to occur. Mutations that led to resistance to IMiDs to a greater extent than CELMoDs in our previous work also demonstrated synergy between Taz and CELMoDs but not IMiDs.

Exploring the mechanism of synergy between Taz and IMiD/CELMoDs we identified a reduction in H3K27me3 at the IRF4 promotor with Taz, consistent with the inhibition of the EZH2 methyltransferase. As H3K27me3 is generally considered a transcriptional repressor it might be expected for this to result in increased IRF4 expression however we did not identify a significant change in IRF4 expression with Taz alone either for RNA (**Figure 6C**) or protein (**Figure 4A mid-left and Figure 6D**). This is consistent with previous studies of single agent EZH2i in myeloma[23, 26] where, at higher concentrations used in our study, IRF4 expression is either unchanged or reduced. We therefore explored the binding of the key IRF4 transcription factors IKZF1 at the IRF4 promotor and enhancer regions. Given our finding of a reduction in focal IKZF1 binding at the *IRF4* promotor and SE

following EZH2i, we propose a model to explain the synergy observed in our study (**Figure 6H**). In resistance control of *IRF4* expression is altered such that the reduction in IKZF1/IKZF3 binding at *IRF4* induced by either Tazemetostat or IMIDs/CELMoDs as single agents, is insufficient to reduce *IRF4* expression. However, the combination of Tazemetostat and IMiDs/CELMoDs work simultaneously to effectively reduce *IRF4* expression, leading to cell death.

Our results provide *in-vitro* evidence to support the study of the combination of Tazemetostat with IMiDs/CELMoDs in relapsed refractory myeloma and suggest the most potent CELMoDs, Iberdomide or Mezigdomide would be the best partner, with these compounds demonstrating the greatest synergy score in cells with good CRBN expression whilst also demonstrating synergy in low CRBN states and in the presence of some CRBN mutations. Interestingly, our combinatorial work also demonstrated synergy between Tazemetostat and dexamethasone supporting the addition of the steroid in combination. The advanced clinical development of both Tazemetostat (FDA approved) and Mezigdomide (in late phase clinical trials) means our findings should be rapidly translatable to the clinic. Independently, a Phase I/II (NCT05372354) trial is currently underway to evaluate the optimal dose of Mezigdomide for just this combination (Mezigdomide, Tazemetostat and dexamethasone) with preliminary results suggesting the optimal dose is 1mg[44]. Initial results from the study, in a very heavily pre-treated patient group (median 5, range 3-14 prior lines of therapy), have reported responses seen in around 2/3 of patients at the optimal dose, with responses seen even in aggressive extramedullary disease states. A Phase II dose expansion is planned to further refine patient response and tolerability.

In summary we provide strong preclinical rationale to support further exploration of EZH2 inhibitor and IMiD/CELMoD combinations in myeloma patients.

References

1. Cancer Research UK, Myeloma Cancer Incidence Trends Over Time, https://www.cancerresearchuk.org/health-professional/cancer-statistics/statistics-by-cancer-type/myeloma/incidence#heading-Three. Accessed 2025, Dec 15.
2. Holstein SA, McCarthy PL. Immunomodulatory Drugs in Multiple Myeloma: Mechanisms of Action and Clinical Experience. Drugs. 2017;77(5):505-520.
3. Ito T, Ando H, Suzuki T, et al. Identification of a primary target of thalidomide teratogenicity. Science. 2010;327(5971):1345-1350.
4. Lu G, Middleton RE, Sun H, et al. The myeloma drug lenalidomide promotes the cereblon-dependent destruction of Ikaros proteins. Science. 2014;343(6168):305-309.
5. Kronke J, Udeshi ND, Narla A, et al. Lenalidomide causes selective degradation of IKZF1 and IKZF3 in multiple myeloma cells. Science. 2014;343(6168):301-305.
6. Pourabdollah M, Bahmanyar M, Atenafu EG, Reece D, Hou J, Chang H. High IKZF1/3 protein expression is a favorable prognostic factor for survival of relapsed/refractory multiple myeloma patients treated with lenalidomide. J Hematol Oncol. 2016;9(1):123.
7. Gooding S, Ansari-Pour N, Towfic F, et al. Multiple cereblon genetic changes are associated with acquired resistance to lenalidomide or pomalidomide in multiple myeloma. Blood. 2021;137(2):232-237.
8. Weber DM, Chen C, Niesvizky R, et al. Lenalidomide plus dexamethasone for relapsed multiple myeloma in North America. N Engl J Med. 2007;357(21):2133-2142.
9. Benboubker L, Dimopoulos MA, Dispenzieri A, et al. Lenalidomide and dexamethasone in transplant-ineligible patients with myeloma. N Engl J Med. 2014;371(10):906-917.
10. Bird S, Pawlyn C. IMiD resistance in multiple myeloma: current understanding of the underpinning biology and clinical impact. Blood. 2023;142(2):131-140.
11. Morelli E, Leone E, Cantafio ME, et al. Selective targeting of IRF4 by synthetic microRNA-125b-5p mimics induces anti-multiple myeloma activity in vitro and in vivo. Leukemia. 2015;29(11):2173-2183.
12. Shaffer AL, Emre NC, Lamy L, et al. IRF4 addiction in multiple myeloma. Nature. 2008;454(7201):226-231.
13. Neri P, Barwick BG, Jung D, et al. ETV4-Dependent Transcriptional Plasticity Maintains MYC Expression and Results in IMiD Resistance in Multiple Myeloma. Blood Cancer Discov. 2024;5(1):56-73.
14. Welsh SJ, Barwick BG, Meermeier EW, et al. Transcriptional Heterogeneity Overcomes Super-Enhancer Disrupting Drug Combinations in Multiple Myeloma. Blood Cancer Discov. 2024;5(1):34-55.
15. Simon JA, Lange CA. Roles of the EZH2 histone methyltransferase in cancer epigenetics. Mutat Res. 2008;647(1-2):21-29.
16. Comet I, Riising EM, Leblanc B, Helin K. Maintaining cell identity: PRC2-mediated regulation of transcription and cancer. Nat Rev Cancer. 2016;16(12):803-810.
17. Duan R, Du W, Guo W. EZH2: a novel target for cancer treatment. J Hematol Oncol. 2020;13(1):104.
18. Croonquist PA, Van Ness B. The polycomb group protein enhancer of zeste homolog 2 (EZH 2) is an oncogene that influences myeloma cell growth and the mutant ras phenotype. Oncogene. 2005;24(41):6269-6280.
19. Pawlyn C, Bright MD, Buros AF, et al. Overexpression of EZH2 in multiple myeloma is associated with poor prognosis and dysregulation of cell cycle control. Blood Cancer J. 2017;7(3):e549.

20. Goldsmith SR, Fiala MA, O'Neal J, et al. EZH2 Overexpression in Multiple Myeloma: Prognostic Value, Correlation With Clinical Characteristics, and Possible Mechanisms. Clin Lymphoma Myeloma Leuk. 2019;19(11):744-750.
21. Mason MJ, Schinke C, Eng CLP, et al. Multiple Myeloma DREAM Challenge reveals epigenetic regulator PHF19 as marker of aggressive disease. Leukemia. 2020;34(7):1866-1874.
22. Ansari-Pour N, Samur M, Flynt E, et al. Whole-genome analysis identifies novel drivers and high-risk double-hit events in relapsed/refractory myeloma. Blood. 2023;141(6):620-633.
23. Alzrigat M, Parraga AA, Agarwal P, et al. EZH2 inhibition in multiple myeloma downregulates myeloma associated oncogenes and upregulates microRNAs with potential tumor suppressor functions. Oncotarget. 2017;8(6):10213-10224.
24. Hernando H, Gelato KA, Lesche R, et al. EZH2 Inhibition Blocks Multiple Myeloma Cell Growth through Upregulation of Epithelial Tumor Suppressor Genes. Mol Cancer Ther. 2016;15(2):287-298.
25. Tremblay-LeMay R, Rastgoo N, Pourabdollah M, Chang H. EZH2 as a therapeutic target for multiple myeloma and other haematological malignancies. Biomark Res. 2018;6:34.
26. Ishiguro K, Kitajima H, Niinuma T, et al. Dual EZH2 and G9a inhibition suppresses multiple myeloma cell proliferation by regulating the interferon signal and IRF4-MYC axis. Cell Death Discov. 2021;7(1):7.
27. Dimopoulos K, Sogaard Helbo A, Fibiger Munch-Petersen H, et al. Dual inhibition of DNMTs and EZH2 can overcome both intrinsic and acquired resistance of myeloma cells to IMiDs in a cereblon-independent manner. Mol Oncol. 2018;12(2):180-195.
28. Ran FA, Hsu PD, Wright J, Agarwala V, Scott DA, Zhang F. Genome engineering using the CRISPR-Cas9 system. Nat Protoc. 2013;8(11):2281-2308.
29. Chrisochoidou Y, Scarpino A, Morales S, et al. Evaluating the impact of CRBN mutations on response to immunomodulatory drugs and novel cereblon E3 ligase modulators in myeloma. Blood. 2025;145(22):2630-2644.
30. Zheng S, Wang W, Aldahdooh J, et al. SynergyFinder Plus: Toward Better Interpretation and Annotation of Drug Combination Screening Datasets. Genomics Proteomics Bioinformatics. 2022;20(3):587-596.
31. Sialana FJ, Roumeliotis TI, Bouguenina H, et al. SimPLIT: Simplified Sample Preparation for Large-Scale Isobaric Tagging Proteomics. J Proteome Res. 2022;21(8):1842-1856.
32. Zhang X, Smits AH, van Tilburg GB, Ovaa H, Huber W, Vermeulen M. Proteome-wide identification of ubiquitin interactions using UbIA-MS. Nat Protoc. 2018;13(3):530-550
33. Keats J, HMCL Characteristics, General Characteristics, https://www.keatslab.org/myeloma-cell-lines/hmcl-characteristics, Accessed 2025, Dec 15.
34. An J, Ponthier CM, Sack R, et al. pSILAC mass spectrometry reveals ZFP91 as IMiD-dependent substrate of the CRL4(CRBN) ubiquitin ligase. Nat Commun. 2017;8:15398.
35. Zhou N, Gutierrez-Uzquiza A, Zheng XY, et al. RUNX proteins desensitize multiple myeloma to lenalidomide via protecting IKZFs from degradation. Leukemia. 2019;33(8):2006-2021.
36. Conery AR, Centore RC, Neiss A, et al. Bromodomain inhibition of the transcriptional coactivators CBP/EP300 as a therapeutic strategy to target the IRF4 network in multiple myeloma. Elife. 2016;5:e19432.
37. Hogg SJ, Motorna O, Cluse LA, et al. Targeting histone acetylation dynamics and oncogenic transcription by catalytic P300/CBP inhibition. Mol Cell. 2021;81(10):2183-2200.
38. Rauluseviciute I, Riudavets-Puig R, Blanc-Mathieu R, et al. JASPAR 2024: 20th anniversary of the open-access database of transcription factor binding profiles. Nucleic Acids Res. 2024;52(D1):D174-D182.
39. Yun S, Cleveland JL. Transcriptional Plasticity Drives IMiD and p300 Inhibitor Resistance in Multiple Myeloma. Blood Cancer Discov. 2024;5(1):5-7.

40. Osada N, Kikuchi J, Iha H, et al. c-FOS is an integral component of the IKZF1 transactivator complex and mediates lenalidomide resistance in multiple myeloma. Clin Transl Med. 2023;13(8):e1364.
41. Alzrigat M, Jernberg-Wiklund H, Licht JD. Targeting EZH2 in Multiple Myeloma-Multifaceted Anti-Tumor Activity. Epigenomes. 2018;2(3):16.
42. Zuo X, Liu D. Mechanism of immunomodulatory drug resistance and novel therapeutic strategies in multiple myeloma. Hematology. 2022;27(1):1110-1121.
43. Caprio C, Sacco A, Giustini V, Roccaro AM. Epigenetic Aberrations in Multiple Myeloma. Cancers (Basel). 2020;12(10):2996.
44. Costa L, Popat R, Siegel D, et al. OA-29 Mezigdomide (MEZI), Tazemetostat (TAZ), and Dexamethasone (DEX) in Patients (pts) With Relapsed/Refractory Multiple Myeloma (RRMM): Preliminary Results From the CA057-003 Trial. Clin Lymphoma Myeloma Leuk. 2024;24:S19.

Figure Legends

Figure 1 IMiD/CELMoD resistance is associated with persistent IRF4 expression

A) Schematic of IMiDs-CRBN-mediated IKZF1/IKZF3 degradation. IMiD binding alters the substrate specificity of CRBN leading to the binding of IKZF1. This results in Ub tagging which marks IKZF1 for degradation via the proteasome. CRBN, cereblon; IKZF1, Ikaros; DDB1, Damage-Specific DNA-Binding Protein 1; CUL4, Cullin-4; RBX1, ring-box protein 1; Ub, ubiquitin. Figure panel created in BioRender. Pawlyn, C. (2025) https://BioRender.com/p91v715.

B) Relative cell viability assessed at Day 5 in MM cell lines treated with indicated IMiD/CELMoD at the concentration of 5µM. Len, Lenalidomide; Pom, Pomalidomide; Iber, Iberdomide.

C) Western blot analysis of indicated proteins in a panel of MM cell lines without treatment.

D) Dose-response curve assessed by cell viability assay in MM cell lines treated with Pomalidomide for 5 days (highest concentration 8uM). Data shown are mean ± SD, n=3 biological replicates.

E) Western blot analysis of indicated proteins in MM cell lines treated with IMiD/CELMoD (10µM) for 5 days.

F) Quantification of IRF4, IKZF1 and IKZF3 expression (normalised to actin) in (E). Data shown are mean ± SD, n=3 biological replicates.

G) Western blot analysis of IRF4 knockdown efficiency.

H) Relative cell viability was assessed at Day 5 in indicated MM cell lines treated with siIRF4. Data shown are mean ± SD, n=3 biological replicates. ***p<0.001.

Figure 2 EZH2i overcomes IMiD/CELMoD resistance, leading to cell death *via* apoptosis

A) Schematic of Tazemetostat-IMiD/CELMoD combination treatment. Cells were first primed in Tazemetostat (0.25µM and 0.125µM for KMS-11 and RPMI-8226 respectively) or DMSO at equivalent concentration for 5 days and then seeded into 96-well plate for IMiD/CELMoD treatment for a further 5 days with the ongoing presence of Tazemetostat/DMSO. Figure panel created in BioRender. Pawlyn, C. (2025) https://BioRender.com/yng6r6g.

B) Dose-response curve assessed by cell viability assay in MM cell lines treated with drug combinations as per A. Pom/Iber highest concentration 8uM. Data shown are mean ± SD, n≥3 biological replicates. **p<0.01.

C) Representative plot of Annexin V/PI staining for detecting apoptosis in KMS-11 primed and Pom treated as per A. Equivalent plot for RPMI-8226 shown in Supplementary Figure S2 and at Day 3 of Pom treatment in Supplementary Figure S3.

D) Quantification of apoptotic induction in KMS-11 and RPMI-8226. Data shown are mean ± SD, n=3 biological replicates. Data shown are mean ± SD, n=3 biological replicates. For statistical comparison the drug combination was compared to pomalidomide monotherapy. *p<0.05; **p<0.01; ***p<0.001.

Figure 3 Tazemetostat is synergistic with IMiD/CELMoD in resistant cell lines

Dose-response curve assessed by cell viability assay in A) indicated MM cell lines treated with multi-dose Tazemetostat-Pomalidomide drug combination and B) KMS-11 cell line treated with multi-dose Tazemetostat and IMiD/CELMoD combinations. Cells were primed in indicated concentration of Tazemetostat or DMSO for 5 days as in Figure 2A and then with combination treatment for 5 days. The highest concentration of Pom used in dose response was 8uM. Data shown are mean ± SD, n>3 biological replicates. Relative cell viability was calculated by normalizing each treatment condition to

the global DMSO control to ensure comparability across treatments and enable synergy score calculation. The mean cell viability for each concentration combination was used to calculate the Bliss synergy score.

Figure 4 Tazemetostat overcomes IMiD/CELMoD resistance in a CRBN-dependent manner

A) Volcano plot for proteomic analysis in KMS-11 treated with Tazemetostat-Pomalidomide drug combination. From left to right: DMSO+DMSO (DD) Vs. DMSO+Pomalidomide (DP), differentially expressed proteins (DEPs) with addition of Pomalidomide without Tazemetostat priming; DMSO+DMSO (DD) Vs. Tazemetostat+DMSO (TD), DEPs with addition of Tazemetostat; DMSO+Pomalidomide (DP) Vs. Tazemetostat+Pomalidomide (TP), DEPs with addition of Pomalidomide in the context of Tazemetostat; DMSO+DMSO (DD) Vs. Tazemetostat+Pomalidomide (TP), DEPs in drug combination compared to the DMSO control; p.val and p.adj were calculated by DEP package[34] in R (4.4.1). Plot shows $\log_{10}$p.val (y-axis) against $\log_2$FC (x-axis). The significant DEPs with p.adj < 0.05 are highlighted (blue = downregulated, green = upregulated). FC, fold change. The data associated with this figure is shared as a Supplementary Appendix.

B) Venn plot of downregulated proteins (DRPs, top) and upregulated proteins (URPs, bottom) when comparing DP compared to DD (DRPs/URPs in Pom) or TP to DD (DRPs/URPs in combination).

C) Western blot analysis of proteins in MM cells lines treated with Tazemetostat-Pomalidomide drug combination. Cells were primed in 0.25uM Tazemetostat for 10 days and treated with 0.5, 2 or 8µM Pomalidomide in KMS-11, and 2 or 8µM Pomalidomide in RPMI-8226 for 24h.

D) Dose-response curve assessed by cell viability assay for drug combination in KMS-11 with CRBN knockout. Cells were primed in indicated concentration of Tazemetostat or DMSO for 5 days and then exposed to Pom/Iber as in Figure 2A. Highest concentration of Pom was 8uM. Data shown are mean ± SD, n=3 biological replicates. * p<0.05; *** p<0.001.

E&F) WB analysis of indicated proteins for the combination in KMS-11 cell line with CRBN knockout. Cells were primed in 0.25µM Tazemetostat for 10 days and treated with 2µM Pomalidomide for 24h. Data shown are mean ± SD, n≥3 biological replicates. *p<0.05, **p<0.01.

Figure 5 Tazemetostat overcomes IMiD/CELMoD resistance in a IRF4-dependent manner

A-C) WB analysis of IRF4 and MYC expression for the drug combinations in KMS-11 cell line with overexpressing IRF4-GFP. Cells were primed in 0.25µM Tazemetostat for 10 days and treated with 2µM Pomalidomide for 24h. Data shown in B and C are quantified from blots, normalised to actin, mean ± SD, n≥3 biological replicates. *p<0.05, **p<0.01.

D) Dose-response curve assessed by cell viability assay for drug combinations in KMS-11 with IRF4 overexpression. Cells were primed in indicated concentration of Tazemetostat or DMSO for 5 days and then exposed to Pom/Iber as in Figure 2A. Highest concentration of Pom was 8uM. Data shown are mean ± SD, n≥3 biological replicates. *p<0.05; ***p<0.001.

Figure 6 Tazemetostat reduces IKZF1 enrichment within the IRF4 promoter

A) qPCR analysis of *IRF4* mRNA expression in cell lines treated with different IMiD/CELMoDs. Data shown are mean ± SD, n≥3 biological replicates. *p<0.05; ***p<0.001.

B) qPCR analysis of *IRF4* mRNA expression in KMS-11 treated with drug combinations. Cells were primed in 0.25µM Tazemetostat for 10 days and treated with 2µM Pomalidomide for 24h. Data shown are mean ± SD, n≥3 biological replicates. *p<0.05; **p<0.01.

C&D) qPCR and WB analysis of *IRF4* mRNA expression in cell lines treated with indicated concentrations of Tazemetostat for 5 days. Data shown are mean ± SD, n=3 biological replicates.

E) ChIP-qPCR analysis of H3K27me3 enrichment within the *IRF4* promoter. MYT1 served as a positive control; Actin served as a negative control. Data shown are mean ± SD, n=3 biological replicates. *p<0.05; **p<0.01.

F) ChIP-qPCR analysis of IKZF1 enrichment within the *IRF4* promoter. Data shown are mean ± SD, n=3 biological replicates.

G) ChIP-qPCR analysis of IKZF1 enrichment within *DUSP22* super-enhancer (SE). Data shown are mean ± SD, n=3 biological replicates.

H) Proposed model of synergistic effect of Tazemetostat-IMiD/CELMoD combination to reduce IRF4 expression in the resistant cell line. Created in BioRender. Pawlyn, C. (2025) https://BioRender.com/n0eekfj

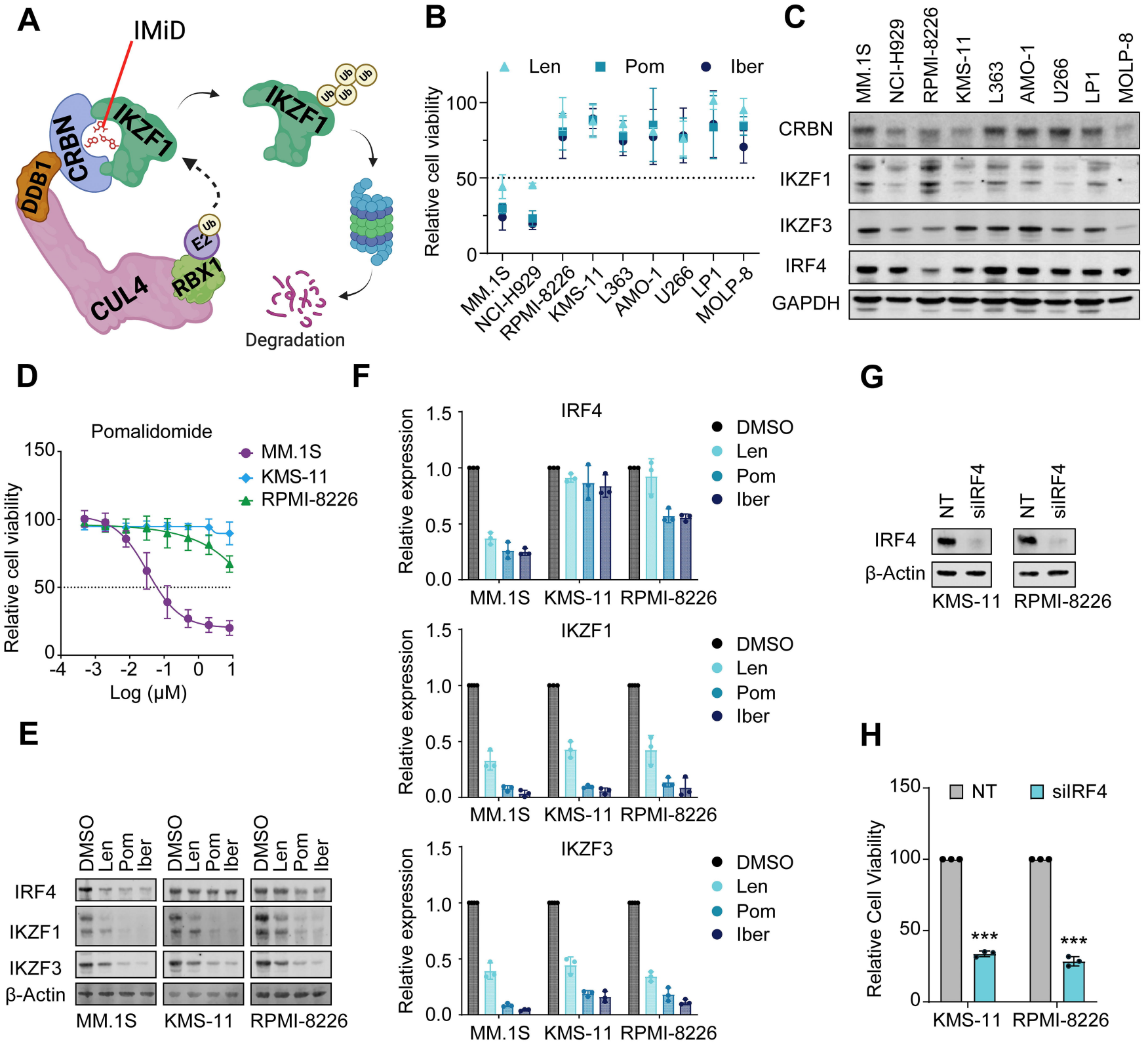
A
IMiD
CRBN
IKZF1
DDB1
CUL4
RBX1
E2
Ub
Degradation
B
Len
Pom
Iber
Relative cell viability
MM.1S
NCI-H929
RPMI-8226
KMS-11
L363
AMO-1
U266
LP1
MOLP-8
C
CRBN
IKZF1
IKZF3
IRF4
GAPDH
D
Pomalidomide
MM.1S
KMS-11
RPMI-8226
Relative cell viability
Log (μM)
E
DMSO
Len
Pom
Iber
IRF4
IKZF1
IKZF3
β-Actin
F
IRF4
IKZF1
IKZF3
Relative expression
G
NT
siIRF4
β-Actin
H
Relative Cell Viability
***

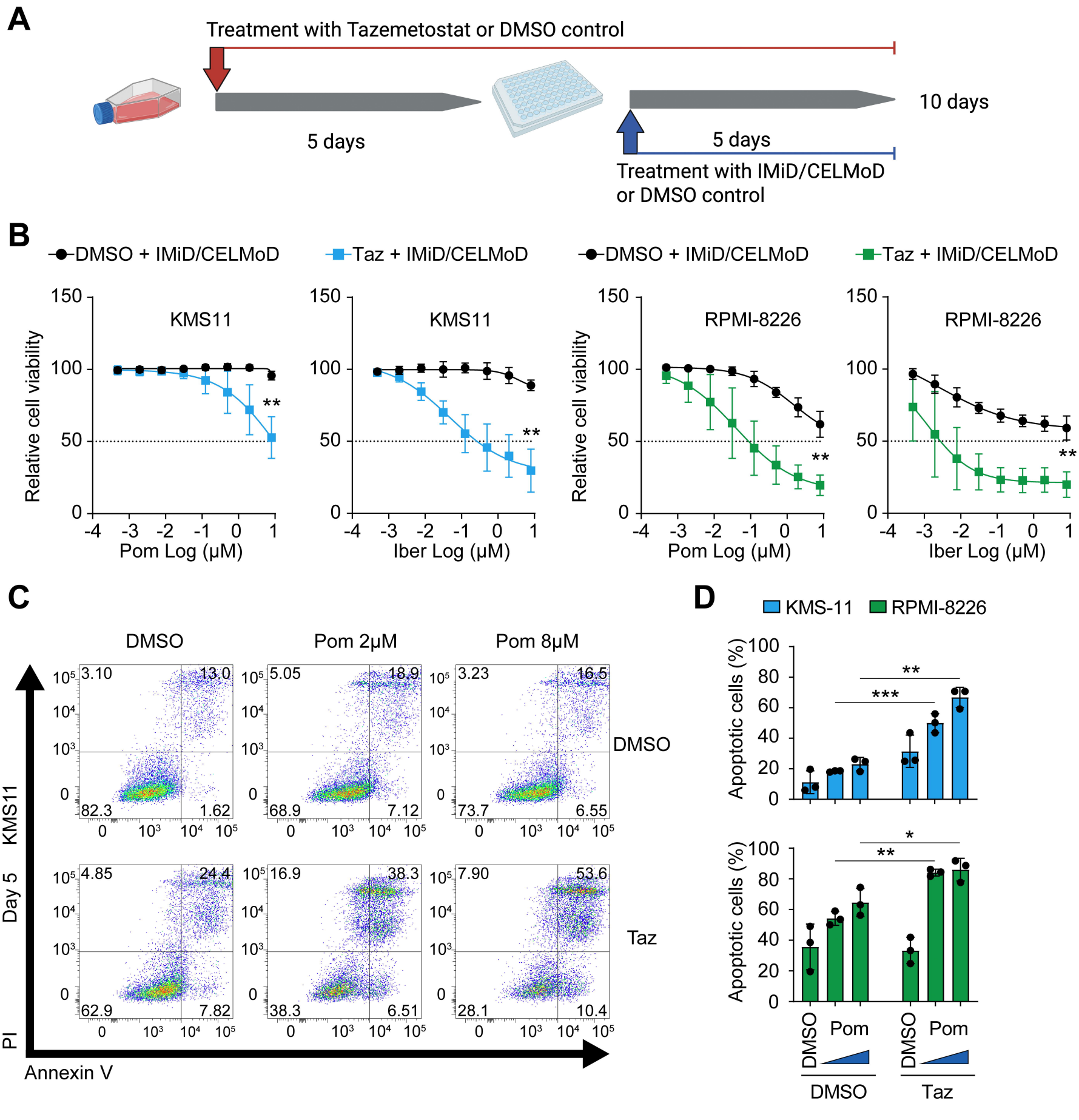
A
Treatment with Tazemetostat or DMSO control
5 days
10 days
5 days
Treatment with IMiD/CELMoD
or DMSO control
B
DMSO + IMiD/CELMoD
Taz + IMiD/CELMoD
DMSO + IMiD/CELMoD
Taz + IMiD/CELMoD
KMS11
KMS11
RPMI-8226
RPMI-8226
Relative cell viability
Relative cell viability
Pom Log (μM)
Iber Log (μM)
Pom Log (μM)
Iber Log (μM)
C
DMSO
Pom 2μM
Pom 8μM
DMSO
Taz
KMS11
Day 5
PI
Annexin V
3.10
13.0
82.3
1.62
5.05
18.9
68.9
7.12
3.23
16.5
73.7
6.55
4.85
24.4
62.9
7.82
16.9
38.3
38.3
6.51
7.90
53.6
28.1
10.4
D
KMS-11
RPMI-8226
Apoptotic cells (%)
Apoptotic cells (%)
DMSO
Pom
DMSO
Pom
DMSO
Taz

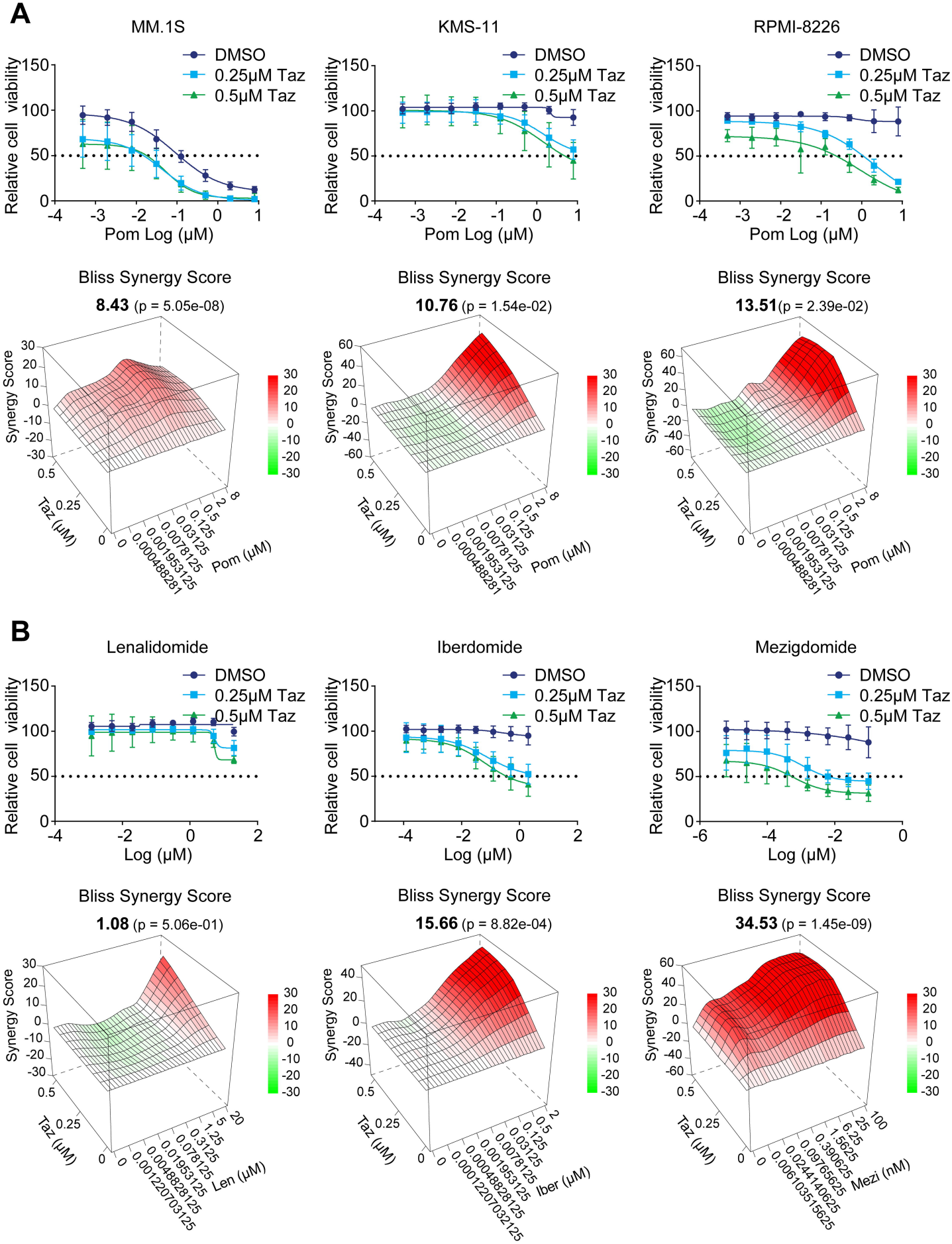
A
MM.1S
KMS-11
RPMI-8226
DMSO
0.25μM Taz
0.5μM Taz
Relative cell viability
Pom Log (μM)
Bliss Synergy Score
8.43 (p = 5.05e-08)
10.76 (p = 1.54e-02)
13.51(p = 2.39e-02)
Synergy Score
Taz (μM)
Pom (μM)
B
Lenalidomide
Iberdomide
Mezigdomide
Log (μM)
1.08 (p = 5.06e-01)
15.66 (p = 8.82e-04)
34.53 (p = 1.45e-09)
Len (μM)
Iber (μM)
Mezi (nM)

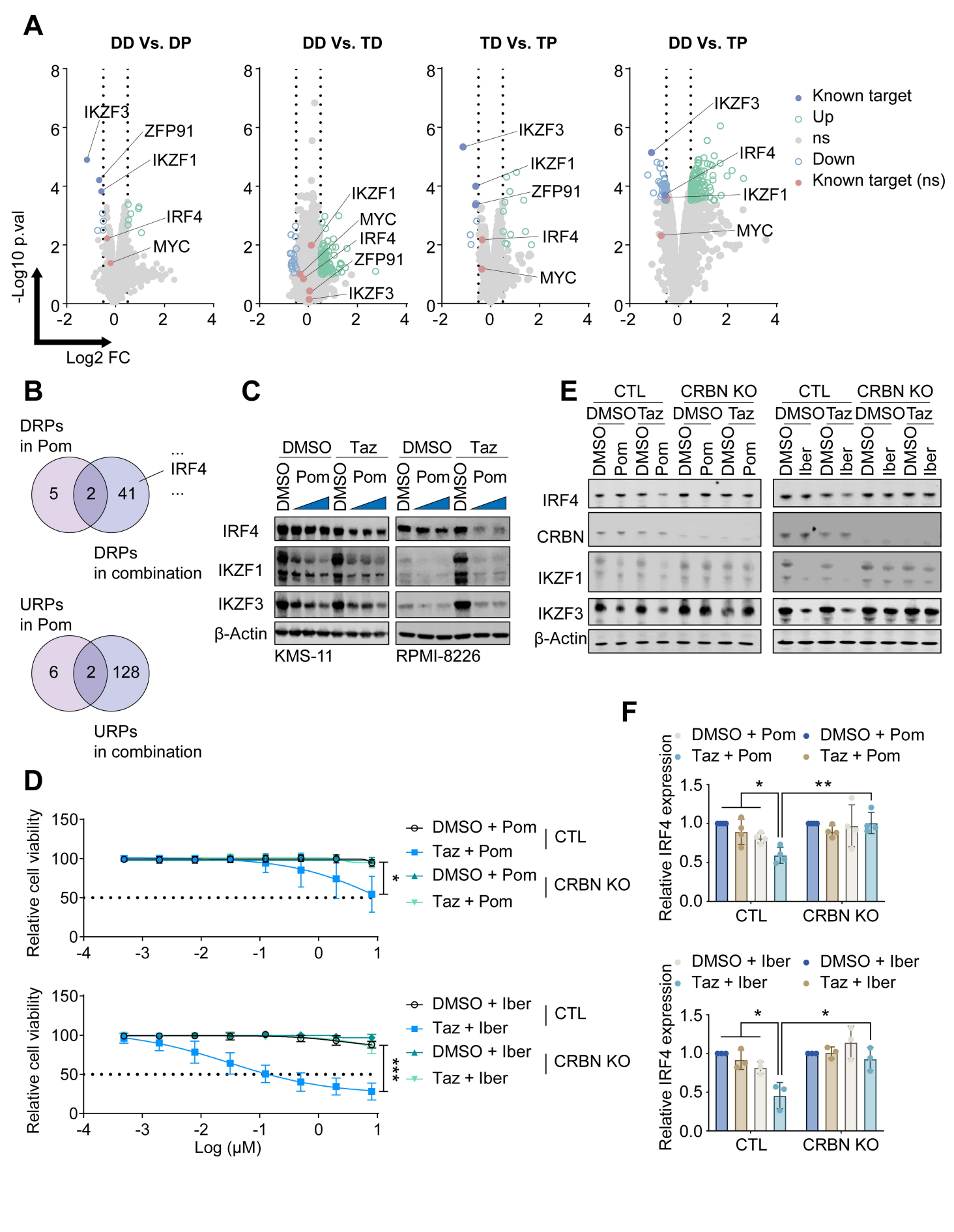
A
DD Vs. DP
DD Vs. TD
TD Vs. TP
DD Vs. TP
IKZF3
ZFP91
IKZF1
IRF4
MYC
-Log10 p.val
Log2 FC
Known target
Up
ns
Down
Known target (ns)
B
DRPs in Pom
5
2
41
...
IRF4
...
DRPs in combination
URPs in Pom
6
2
128
URPs in combination
C
DMSO
Taz
Pom
IRF4
IKZF1
IKZF3
β-Actin
KMS-11
RPMI-8226
E
CTL
CRBN KO
DMSO
Pom
Iber
IRF4
CRBN
IKZF1
IKZF3
β-Actin
D
Relative cell viability
DMSO + Pom
Taz + Pom
DMSO + Pom
Taz + Pom
CTL
CRBN KO
DMSO + Iber
Taz + Iber
DMSO + Iber
Taz + Iber
Log (μM)
F
Relative IRF4 expression
DMSO + Pom
Taz + Pom
DMSO + Iber
Taz + Iber
CTL
CRBN KO

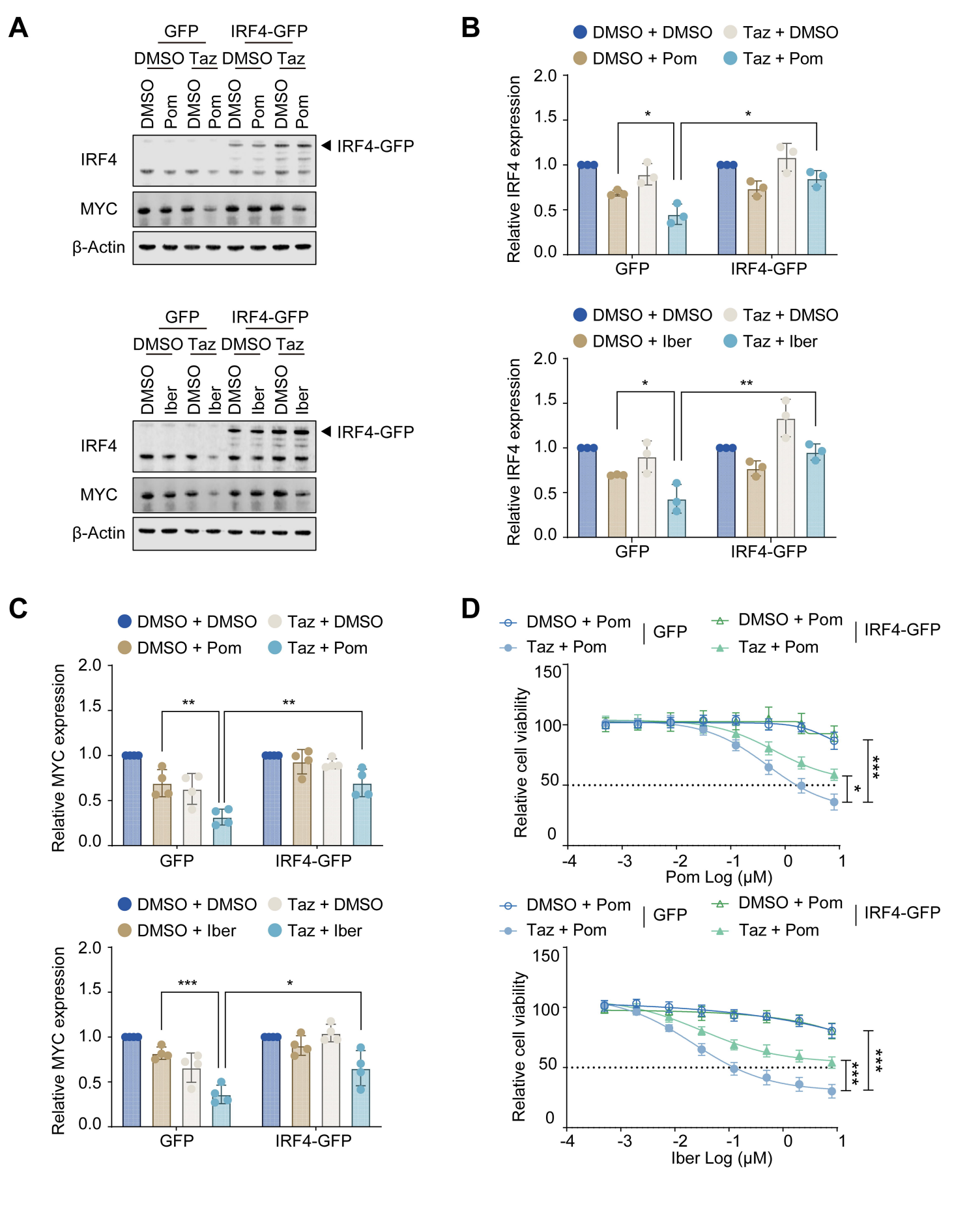
A
GFP
IRF4-GFP
DMSO Taz DMSO Taz
DMSO Pom DMSO Pom DMSO Pom DMSO Pom
IRF4
MYC
β-Actin
◀ IRF4-GFP
GFP
IRF4-GFP
DMSO Taz DMSO Taz
DMSO Iber DMSO Iber DMSO Iber DMSO Iber
IRF4
MYC
β-Actin
◀ IRF4-GFP
B
DMSO + DMSO
Taz + DMSO
DMSO + Pom
Taz + Pom
Relative IRF4 expression
2.0
1.5
1.0
0.5
0.0
*
*
GFP
IRF4-GFP
DMSO + DMSO
Taz + DMSO
DMSO + Iber
Taz + Iber
Relative IRF4 expression
2.0
1.5
1.0
0.5
0.0
*
**
GFP
IRF4-GFP
C
DMSO + DMSO
Taz + DMSO
DMSO + Pom
Taz + Pom
Relative MYC expression
2.0
1.5
1.0
0.5
0.0
**
**
GFP
IRF4-GFP
DMSO + DMSO
Taz + DMSO
DMSO + Iber
Taz + Iber
Relative MYC expression
2.0
1.5
1.0
0.5
0.0
***
*
GFP
IRF4-GFP
D
DMSO + Pom
Taz + Pom
GFP
DMSO + Pom
Taz + Pom
IRF4-GFP
Relative cell viability
150
100
50
0
*
***
-4
-3
-2
-1
0
1
Pom Log (μM)
DMSO + Pom
Taz + Pom
GFP
DMSO + Pom
Taz + Pom
IRF4-GFP
Relative cell viability
150
100
50
0
***
***
-4
-3
-2
-1
0
1
Iber Log (μM)

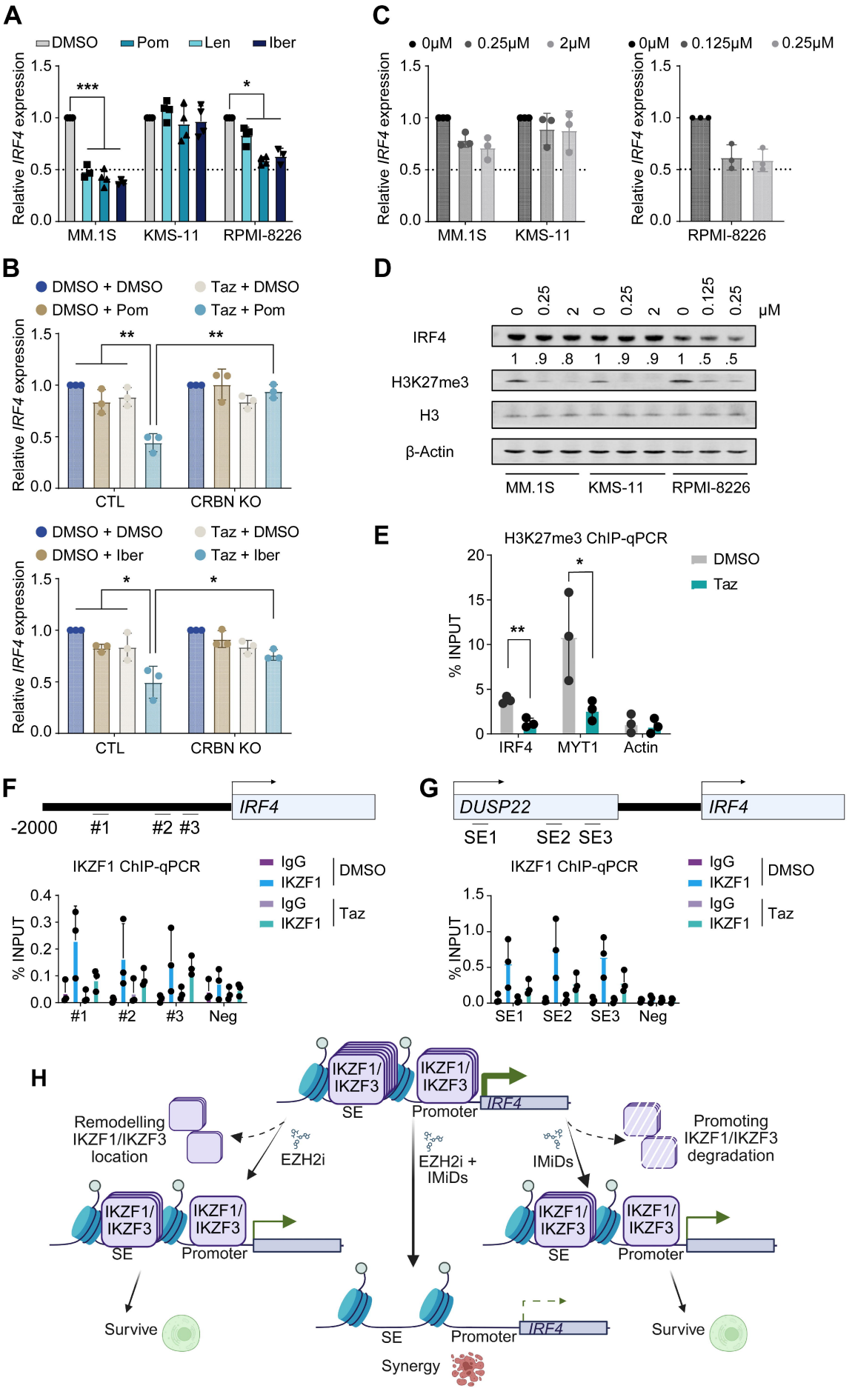
A
DMSO
Pom
Len
Iber
Relative IRF4 expression
MM.1S
KMS-11
RPMI-8226
B
DMSO + DMSO
Taz + DMSO
DMSO + Pom
Taz + Pom
CTL
CRBN KO
DMSO + Iber
Taz + Iber
C
0μM
0.25μM
2μM
0.125μM
D
IRF4
H3K27me3
H3
β-Actin
μM
E
H3K27me3 ChIP-qPCR
% INPUT
IRF4
MYT1
Actin
F
IRF4
-2000
#1
#2
#3
IKZF1 ChIP-qPCR
IgG
IKZF1
Neg
G
DUSP22
SE1
SE2
SE3
H
IKZF1/ IKZF3
SE
Promoter
Remodelling IKZF1/IKZF3 location
EZH2i
EZH2i + IMiDs
IMiDs
Promoting IKZF1/IKZF3 degradation
Survive
Synergy

SUPPLEMENTARY MATERIAL

EZH2 inhibition overcomes immunomodulatory drug resistance in multiple myeloma via a cereblon-dependent pathway

Yigen Li[1]*, Amy Wilson[1]*, Yakinthi Chrisochoidou[1], Shannon Martin[1], Sarah Bird[1,2], Salomon Morales[1], Marc Leiro[1], Zuza Kozik[1], Nicholas T. Crump[3], Theodoros I. Roumeliotis[1], Jyoti Choudhary[1], Charlotte Pawlyn[1,2]

1. The Institute of Cancer Research, London
2. The Royal Marsden Hospital NHS Foundation Trust, London
3. Hugh and Josseline Langmuir Centre for Myeloma Research, Centre for Haematology, Department of Immunology and Inflammation, Imperial College London, London
*Joint first authors

Contents

Supplementary Methods

Cell lines and compounds

MM.1S-Iberdomide-Resistant cell line was generated by long-term low-dose exposure of MM.1S to Iberdomide (0.01uM). Resistance was acquired gradually, with full resistance by 12 weeks of incubation associated with decreased CRBN protein expression. Cell lines underwent whole exome sequencing with no mutations in CRBN identified. Cell identity was confirmed using STR typing (Eurofins) and confirmed mycoplasma negative (MycoStrip, InvivoGen).

Lenalidomide and Pomalidomide were purchased from Fluorochem Ltd. Tazemetostat (EPZ-6438), Iberdomide and Mezigdomide were synthesized in-house using literature procedures.

Small interfering RNA (siRNA)

SMARTPool of siRNAs targeting Human IRF4 (E-019668-01-0005) and Non-targeting Pool (NT, D-001910-10-05) were purchased from Horizon (UK). Transfection was performed using DharmaFECT 1 (T-2001-01), following manufacturer's instructions. The final concentration of siRNAs was 100nM.

Western blot analysis

Cells were lysed in 2% SDS buffer. Protein concentration was measured by BCA protein assay (23225, Thermo Fisher Scientific). Equal amounts of protein were separated by sodium dodecyl sulfate–polyacrylamide gel electrophoresis and transferred onto PVDF membrane (88518, Thermo Scientific), followed by immunoblot analysis. Antibodies used in this study were as follows: CRBN (71810, CST), IKZF1 (14859, CST), IKZF3 (15103, CST), β-Actin (A5441, SIGMA-ALDRICH), IRF4 (15106, CST). Western blots were visualized by Odyssey Fc Imager (LI-COR) using IRDye Infrared Dyes as secondary antibody. Densitometry analysis was performed using ImageJ (NIH, USA).

RNA extraction and quantitative RT-PCR analysis

Total RNA was extracted using RNeasy Plus Mini Kit (74134, QIAGEN) according to the manufacturer's instructions. First-strand cDNA was synthesized using cDNA Reverse Transcription Kit (10400745, Thermo Fisher Scientific). Expression of mRNA targets was measured using TaqMan Gene Expression Assays and GAPDH was served as housekeeping. The reaction was performed on ABI 7500 Real-Time PCR system using TaqMan Fast Advanced Master Mix (4444963, ABI) and primers for GAPDH (Hs99999905_m1) and IRF4 (Hs01056533_m1). The relative changes of gene expression were calculated according to the $2^{-\Delta\Delta CT}$ quantification method.

Apoptosis analysis

Apoptosis was determined using APC-Annexin V (550475, BD Biosciences) according to the manufacturer's instructions. Cells were primed in EZH2i for 5 days and then treated with IMiDs. After 72h and 120h, cells were harvested and stained with APC-Annexin V for 15min at room

temperature and PI for 5min at room temperature. Annexin/PI-positive cells were analyzed using flow cytometry (LSR II, BD Biosciences) within 1h.

Chromatin immunoprecipitation (ChIP)-qPCR assay

KMS-11 cells were incubated in 2μM Tazemetostat or DMSO for 10 days. Then cells were fixed with 1% formaldehyde solution for 15 min and incubated with 125 nM glycine for 5 min. DNA fragments ranging from 200 to 500 bp were generated using sonication. Antibodies including H3K27me3 (61017, ACTIVE MOTIF), IKZF1 (39356, ACTIVE MOTIF) and IgG (2729, CST) were employed for specific immunoprecipitation. qPCR was used to analyze the precipitated DNA. Primers used for detecting indicated enrichment were as follows, H3K27me3 (F, ACTCTCAGTTTCACCGCTCG; R, CTCCGGGTCCTCTCTGGTAT); MYT1 (F, ACAAAGGCAGATACCCAACG; R, GCAGTTTCAAAAAGCCATCC); ACTB (71023, Active Motif); IKZF1 (#1F, AGTTGCAGGTTGACCTACGG; #1R, AGCTTTCACCCGTTGAGCTT; #2F, GCCCCCATCTCTTTCATGCT; #2R, CCTCTCCGCGGTGTTTAGAG; #3F, GGACCATTCCTCCGTCTTCC; #3R, AATGCGAATCTCGCCTTTGC; SE1 F, CAGGTGACCTTCAGAGTTTGT; SE1 R, CCAGGTCTCTCCCATCCTATTA; SE2 F, GCCTCTCCTTACAACTGAAGAC; SE2 R, CAGGTGACTGCTCAAGTACAG; SE3 F, GCAGAAAGCCTATTCCAGAGAG; SE3 R, ATCCATGATCTCTCCCTCCTAC); Neg (F, CGTGGCTATGTTTGCTTGGG; R, AGCAGGCCTCTTGGTTGTTT).

Proteomics

Briefly, LC-MS analysis was performed with an UltiMate 3000 RSLCnano system (Thermo Fisher Scientific) coupled to the Orbitrap Fusion Lumos mass spectrometer (Thermo Fisher Scientific) using a 25cm capillary column (Waters, nanoE MZ PST BEH130 C18, 1.7μm, 75μm × 250mm) over a 100min gradient 5%-35% of mobile phase B composed of 80% acetonitrile, 0.1% formic acid. Peptides were preconcentrated onto an Acclaim PepMap 100, 100μm × 2cm C18, 5μm trapping column at 10μL/min of 0.1% TFA and the analytical column was connected to an EASY-Spray emitter (ES991, Thermo Fisher Scientific). MS spectra were collected at Orbitrap mass resolution of 120,000 and precursors were targeted for HCD fragmentation in the top speed mode (3 sec) with collision energy 36% and Orbitrap detection with a resolution of 45,000. Targeted precursors were dynamically excluded from further activation for 45 seconds with 10ppm mass tolerance.

The Sequest HT node in Proteome Discoverer 3.0 (Thermo) was used to search the raw mass spectra against a FASTA file containing reviewed UniProt Homo sapiens entries. The precursor mass tolerance was set at 20ppm and the fragment ion mass tolerance at 0.02Da with up to 2 trypsin missed-cleavages allowed. TMTpro at N-terminus/K and Carbamidomethyl at C were defined as static modifications. Dynamic modifications were oxidation of M and deamidation of N/Q. Peptide confidence was estimated with the Percolator node and peptide FDR was set at 0.01 based on target-decoy search. Only unique peptides were used for quantification, considering protein groups for peptide uniqueness. Peptides with average reporter signal-to-noise greater than 3 were used for protein quantification.

Supplementary Figures

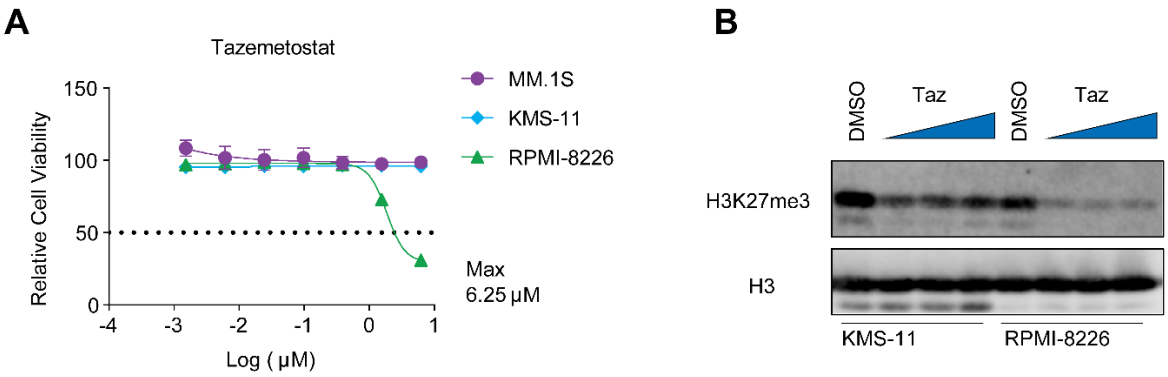

Figure S1 Optimization of Tazemetostat concentration used for priming
A) Dose-response curve in MM cell lines treated with Tazemetostat (highest 6.25µM) for 5 days.
B) WB analysis of H3K27me3 with titration of Tazemetostat concentration (0.5, 1, 2µM) for 5 days.

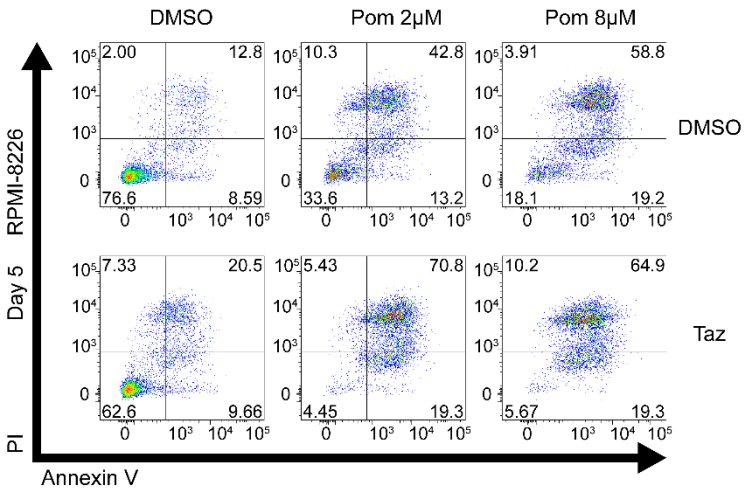

Figure S2 Tazemetostat-Pomalidomide induces apoptosis in RPMI-8226
Representative plot of Annexin V/PI staining for detecting apoptosis in RPMI-8226. Cells were primed in 0.125μM Tazemetostat or DMSO for 5 days and then treated with indicated Pomalidomide combination (alongside Tazemetostat/DMSO) for 5 days. Equivalent plot for KMS-11 is shown in Figure 2C.

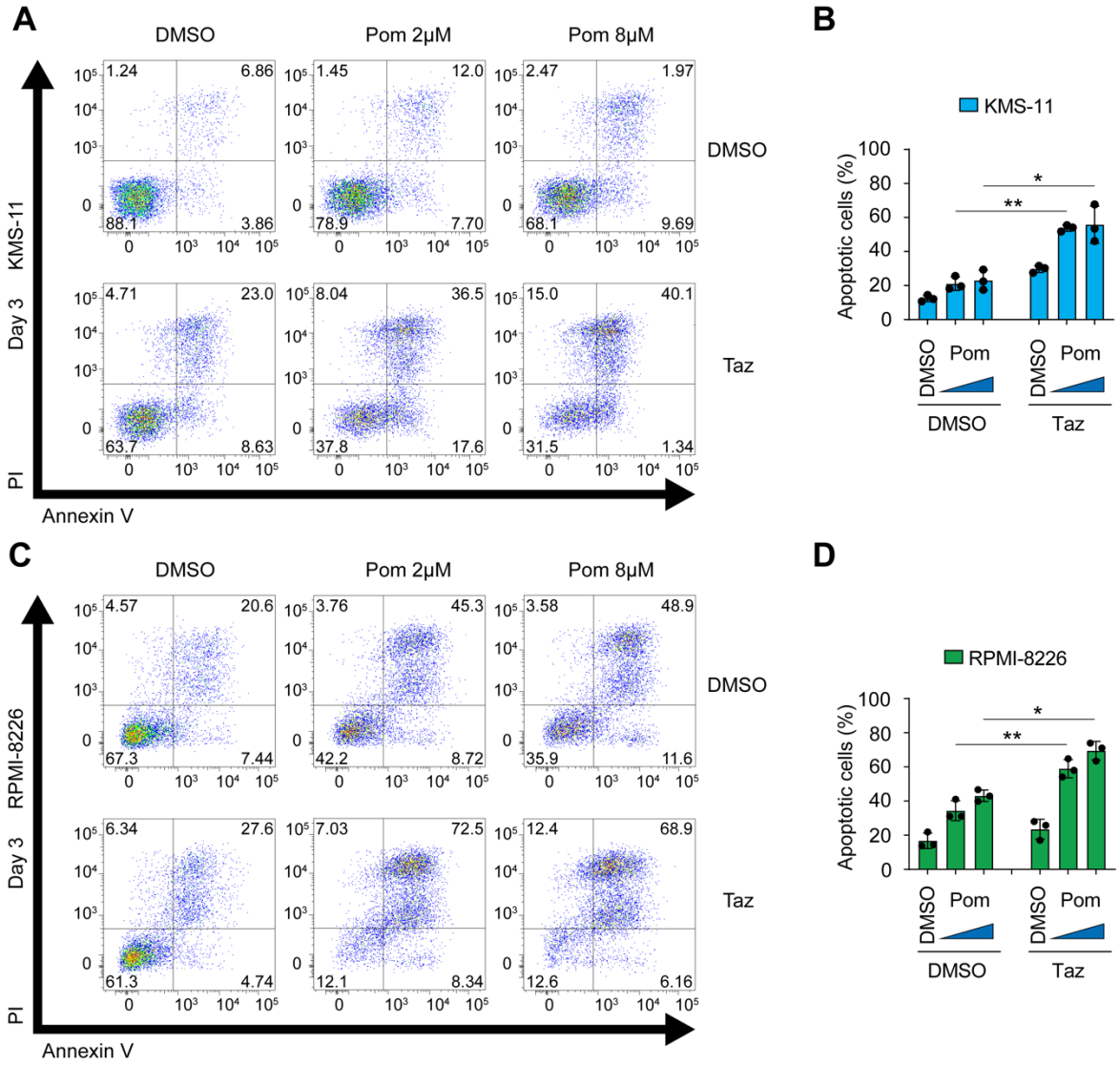

Figure S3 Tazemetostat-Pomalidomide induces apoptosis in KMS-11 and RPMI-8226

Representative plot and quantification of Annexin V/PI staining for detecting apoptosis in KMS-11 (A&B) and RPMI-8226 (C&D), which were primed in 0.25 or 0.125μM Tazemetostat respectively for 5 days and then treated with indicated Pomalidomide concentration (alongside Tazemetostat/DMSO) for 3 days. For statistical comparison the drug combination was compared to pomalidomide monotherapy. Data shown are mean ± SD, n=3 biological replicates. *p<0.05; **p<0.001.

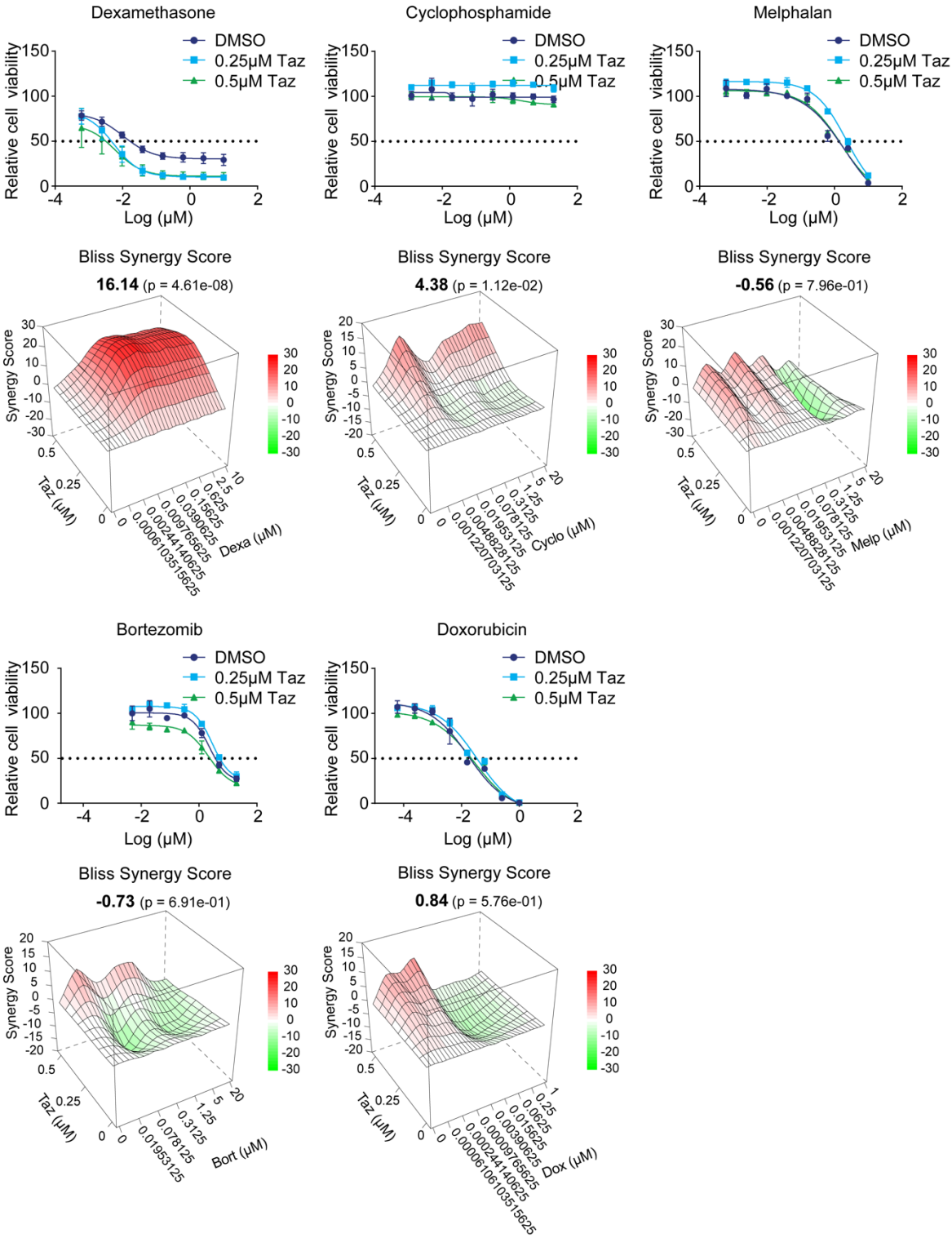

Figure S4 Tazemetostat is synergistic with Dexamethasone

Dose-response curve in KMS-11 treated with multi-dose drug combinations. Data shown are mean ± SD, n=3 biological replicates. The mean cell viability was used to calculate the synergy score.

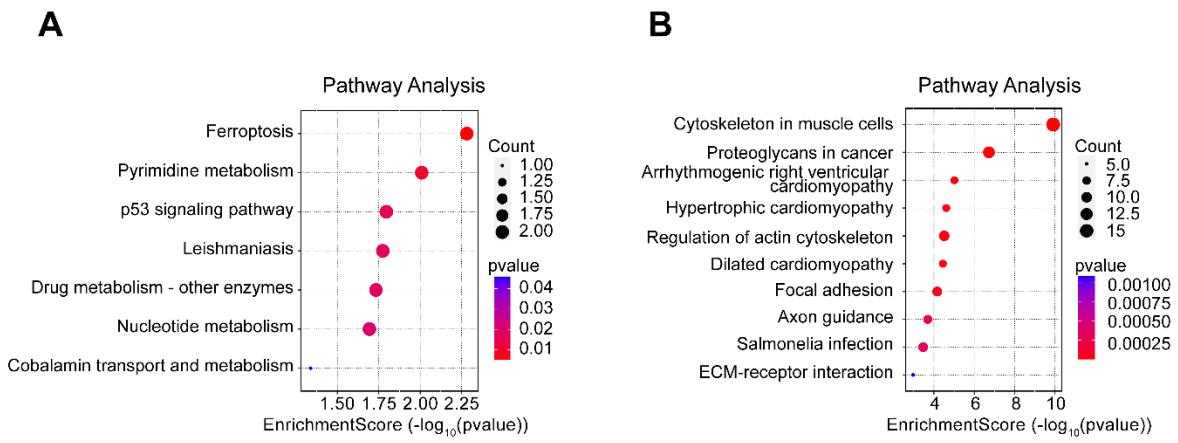

Figure S5 KEGG pathway analysis

A) KEGG pathway enrichment analysis for downregulated proteins with the drug combination (Tazemetostat and Pomalidomide).

B) KEGG pathway enrichment analysis for upregulated proteins with the drug combination (Tazemetostat and Pomalidomide).

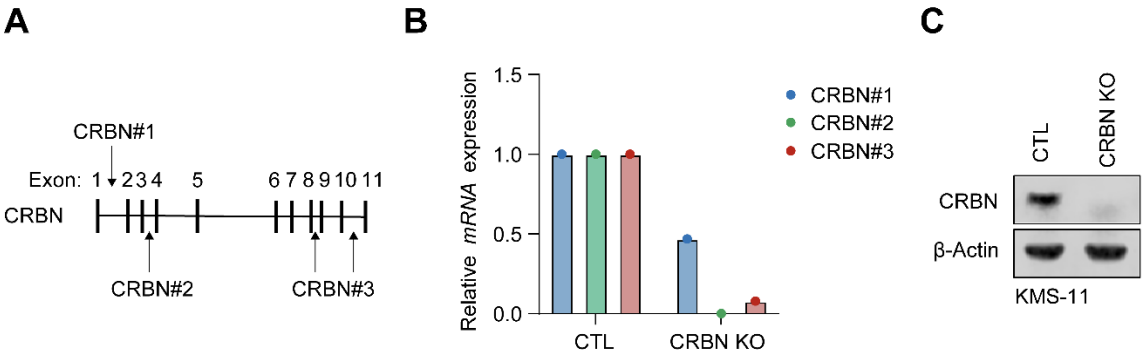

Figure S6 Validation of CRBN KO in KMS-11

A) Schematic of TaqMan probes targeting CRBN. CRBN#1 (HS01020593): Interrogated sequence in the boundaries of exons 1 & 2; CRBN#2 (HS00372266): Interrogated sequence in the boundaries of exons 3 & 4; CRBN#3 (HS00372271): Interrogated sequence in the boundaries of exons 8 & 9, and exons 10 & 11.

B&C) qPCR and WB analysis for validation of CRBN KO in KMS-11.

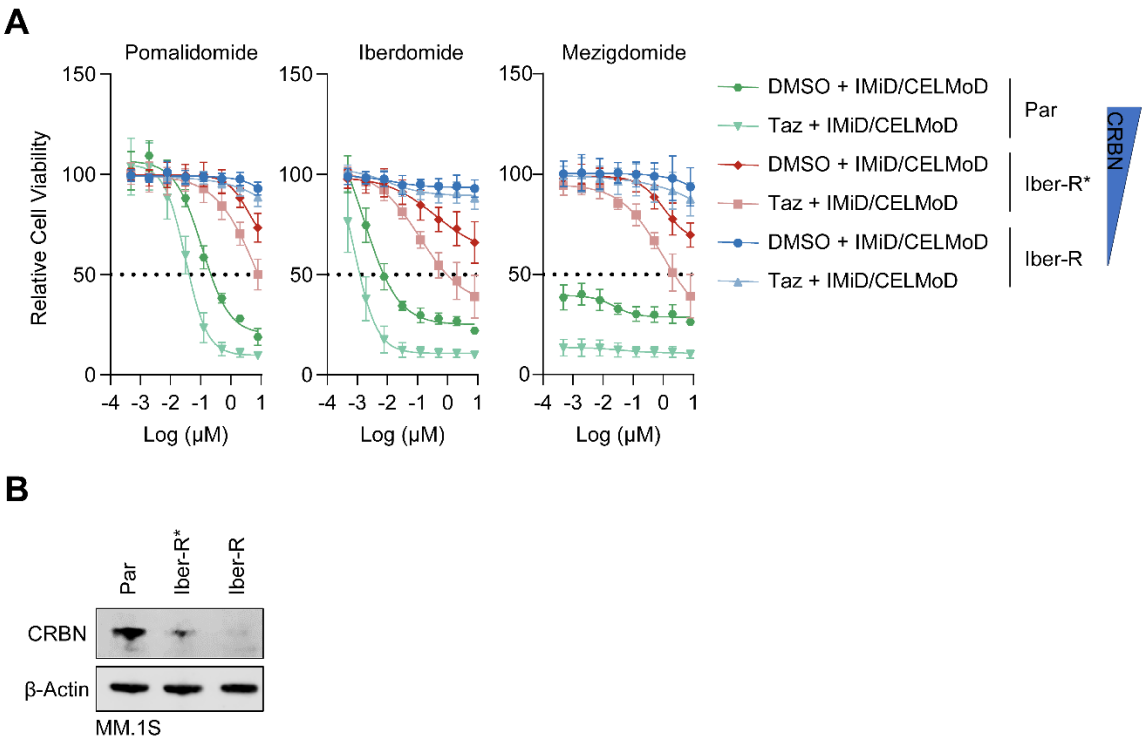

Figure S7 Tazemetostat overcoming IMiD/CELMoD resistance is CRBN-dependent

A) Dose-response (highest 8μM) curve assessed by cell viability assay for drug combinations in MM.1S (Iber-R) cell line, which developed acquired resistance after exposure to Iberdomide (0.01μM) for 6 months. Iber-R*, which retains residual CRBN expression as shown in (B), is not completely resistant to Iberdomide. Data shown are mean ± SD, n ⩾ 4 biological replicates.

B) WB analysis of CRBN expression in MM.1S Iber-R cell line, compared to the parental MM.1S cell line. Iber-R*, cell lines with residual CRBN expression.

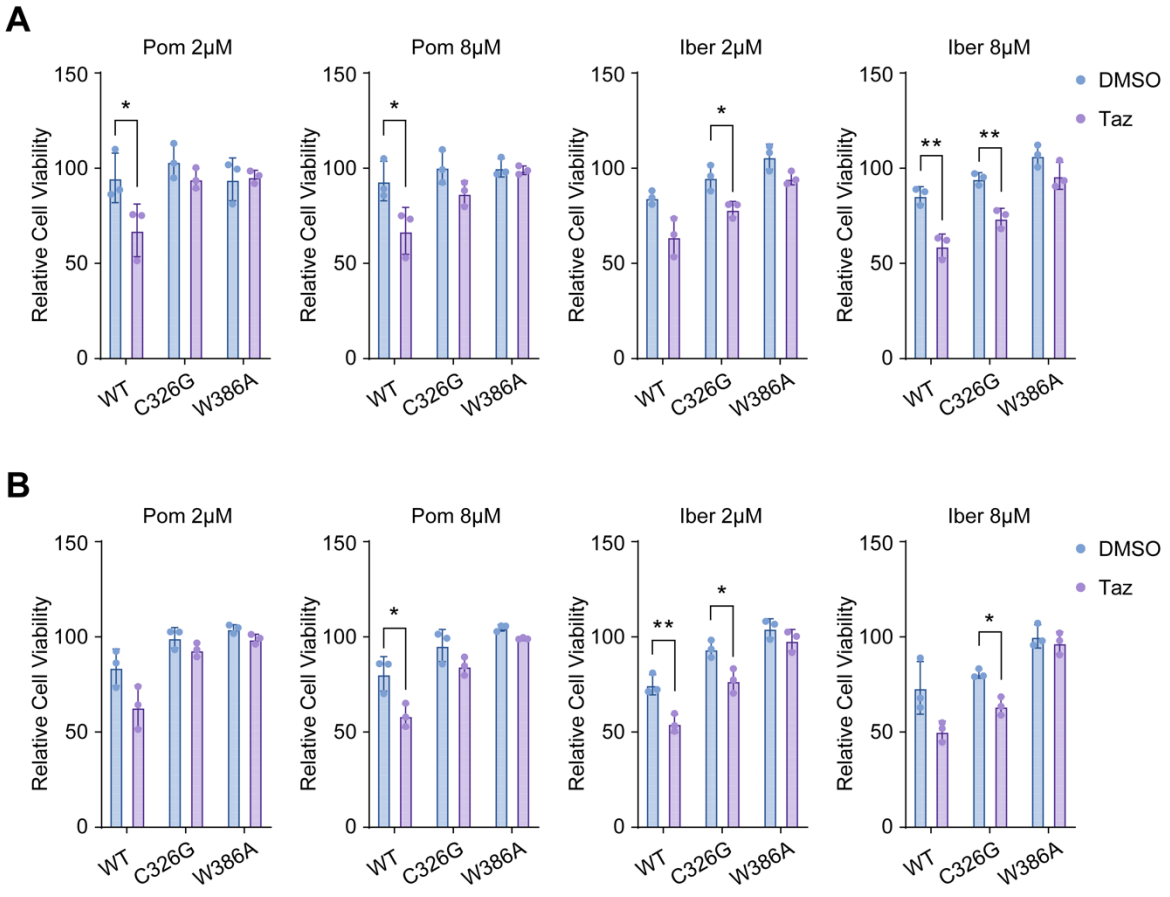

Figure S8 Tazemetostat and IMiD/CELMoD synergy depends on functional CRBN
Cell viability measured in CRBN mutants KMS-11 (A) or MM.1S (B) cell lines, which were primed in 0.25μM Tazemetostat for 5 days and treated with indicated concentrations of IMiD/CELMoD as per Figure 2A. Data shown are mean ± SD, n=3 biological replicates. *p<0.05; **p<0.001.

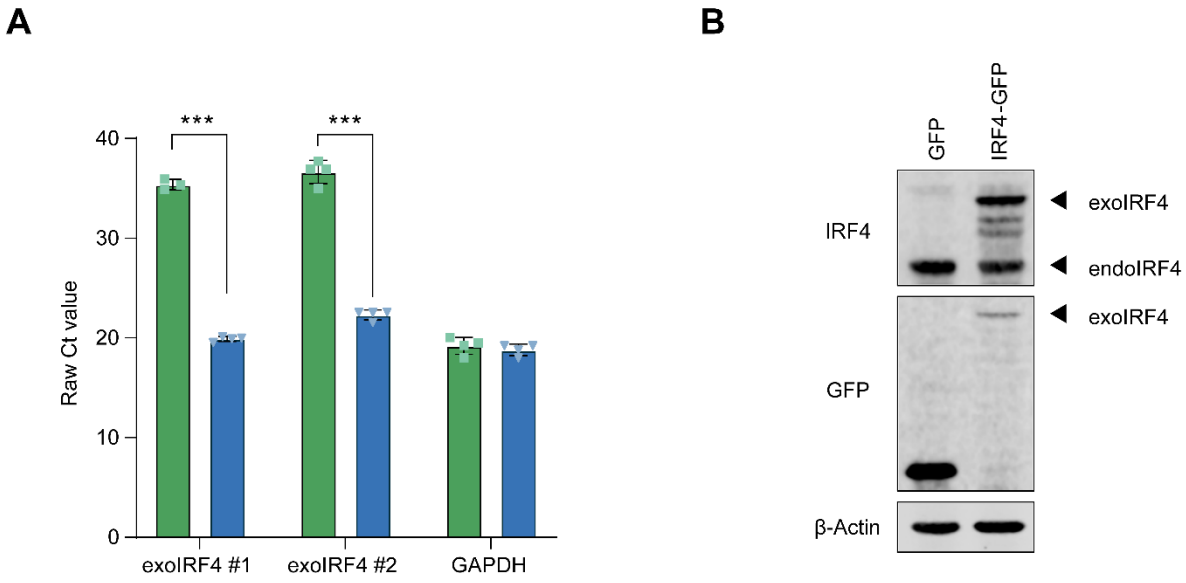

Figure S9 Validation of exogenous IRF4 overexpression

A) qPCR analysis for detecting exogenous *IRF4* in KMS-11. Primers were designed to specifically target exogenous *IRF4* (codon optimised) mRNA sequence. Raw Ct values were used to indicate IRF4 overexpression. Data shown are mean ± SD, n⩾3 biological replicates. ***p<0.001.

B) WB analysis for detecting exogenous and endogenous IRF4 expression in KMS-11.

Supplementary Tables

Table S1 IC50 of MM cell lines treated with indicated IMiD/CELMoD

	Len (μM)	Pom (μM)	Iber (μM)
MM.1S	3.3698 ± 3.4057	0.1642 ± 0.0550	0.0038 ± 0.0011
NCI-H929	3.4057 ± 0.3738	0.1387 ± 0.1192	0.0076 ± 0.0005
RPMI-8226	>20	>20	>20
KMS-11	>20	>20	>20
L363	>20	>20	>20
AMO-1	>20	>20	>20
U266	>20	>20	>20
LP1	>20	>20	>20
MOLP-8	>20	>20	>20
The maximum drug concentration is 20μM.			

Table S2 MM cell lines characteristics

Data from https://www.keatslab.org/myeloma-cell-lines/hmcl-characteristics

Public Name	Sex	Ancestry	Clinical Heavy Chain	Clinical Light Chain	Canonical Translocations	TP53
MM.1S	Female	Africa	IgA	Lambda	t(14:16) + t(8;14)	Wt
NCI-H929	Female	Europe	IgA	Kappa	t(4;14)	Wt
RPMI-8226	Male	Africa	IgG	Lambda	t(16;22) + t(8;22)	E285K - Homo (cc)
KMS-11	Female	East Asia	IgG	Kappa	t(4;14) + t(8;14) + t(14;16)	
L363	Female	Europe	IgG	Lambda	t(20;22)	S261T - Homo
AMO-1	Female	East Asia	IgA	Kappa	t(8;14)	Wt
U266	Male	Europe	IgE	Lambda	t(11;14)	A161T - Homo (cc)
LP-1	Female	Europe	IgG	Lambda	t(4;14) + t(8;14)	E286K - Homo (cc)
MOLP-8	Male	East Asia	IgD	Lambda	t(11;14)	

Supplementary Appendix

Data for Figure 4: Supplementary Appendix_DEP Data for Figure 4.xlsx